

Undulation Amplitude of a Fluid Membrane Immersed in a Near-Critical Binary Fluid Mixture beyond the Regime of the Gaussian Model with Weak Preferential Attraction

Youhei Fujitani*

School of Fundamental Science and Technology, Keio University, Yokohama 223-8522, Japan

(Dated: October 13, 2015)

The shape fluctuation of an almost planar fluid membrane immersed in a near-critical binary fluid mixture is considered within the linear approximation with respect to its amplitude. It is usual that one component is preferably attracted by the membrane, which generates the additional stress including the osmotic pressure. By using the Gaussian free-energy functional and assuming the preferential attraction to be sufficiently weak, the present author recently pointed out theoretically that the ambient near-criticality tends to suppress the mean square amplitude; the generated restoring force has the wavenumber-squared dependence and becomes larger with the correlation length far from the membrane. In this paper, we first calculate this equal-time correlation in the Gaussian model beyond the regime of the weak preferential attraction. The result shows that the suppression effect continues although the numerical factor of the restoring force is effectively reduced to about half. Second, assuming the critical fraction far from the membrane, we calculate by using the renormalized local functional theory. The result turns out to be almost equal to the corresponding result in the Gaussian model if the correlation length is regarded as the one near the membrane. Thus, the suppression effect reaches a plateau as the temperature approaches the critical one, which cannot be expected by the Gaussian model.

PACS numbers: 68.15.+e, 05.40.-a, 05.70.Jk, 47.57.-s

I. INTRODUCTION

A fluid membrane is a two-dimensional fluid with the bending rigidity [1, 2], and is usually composed of one layer or two layers of amphiphilic molecules. A typical example is the lipid-bilayer membrane in the biomembrane [3]; the polar head groups are arranged outwards and in contact with the aqueous environments. The thermal undulation, or shape fluctuation, of the membrane at the equilibrium can explain the flicker phenomenon of red blood cells [4]. When the cell is not swollen, the mean lateral tension of the membrane vanishes at the equilibrium because the membrane area is determined so that the free energy is minimized [5–7]. In such a tensionless membrane, the undulation amplitude is determined by the bending rigidity and becomes scale invariant. This causes decrease in the effective bending rigidity as the membrane area is larger; a sufficiently large membrane loses its orientation to become floppy [8–10]. The oil-water interface can have the same property when saturated by surfactants [11, 12]. The bilayer membrane composed of sodium dodecyl-sulfate, pentanol, and water has inverted polarity; the non-polar chains are arranged outwards in some organic solvent [13, 14]. Fluid membranes are often stacked regularly and the resultant lamellar structure can work as a photonic device [15]; the interaction between them partly comes from steric hindrance due to

the undulation [8, 9, 16].

Suppose an impurity immersed in a near-critical binary fluid mixture. It is usual that one component is preferably attracted by the impurity because the two components differently interacts with the impurity surface. When the interaction is short-ranged, the difference is represented by the surface field. This name comes from the corresponding quantity of the Ising model in a finite lattice, as stated later. The preferential attraction causes the adsorption layer of the preferred component, which becomes more remarkable as the mixture approaches the critical point [17–21]. The resultant gradient of the concentration difference between the two components generates additional stress including the osmotic pressure and can influence the dynamics of the impurity sufficiently large as compared with the correlation length [22]. The impurity can be a colloidal particle [23–26], the drag coefficient of which deviates from the Stokes law owing to the ambient near-criticality combined with the preferential attraction [27].

The impurity can be a fluid membrane. By using the Gaussian free-energy functional and assuming the surface field to be sufficiently weak, the present author recently calculated the equilibrium average of the undulation amplitude of a fluid membrane immersed in a near-critical binary fluid mixture [28]. To calculate this equal-time correlation, we cannot take the ensemble average naively by regarding the ambient mixture as a heat and particle bath. The chemical potential of the

*Electronic address: youhei@appi.keio.ac.jp

mixture is not homogeneous but changed locally by the membrane motion, which drives flow to change the local fraction in the mixture. The mixture part closely linked with the membrane cannot be regarded as a bath, unlike the mixture part far from the membrane. In Ref. 28, the present author utilizes the dynamics in the limit of no dissipation to take into account the influence of the former part. The result shows that the restoring force due to the ambient near-criticality tends to suppress the undulation, has the wavenumber-squared dependence, and becomes larger with the correlation length far from the membrane. However, the surface field is not always weak and the Gaussian model ceases to be valid when the mixture is very close to the critical point. In this paper, we calculate the mean square amplitude beyond the regime of the Gaussian model and a weak surface field. We here also utilize the dynamics in the limit of no dissipation; the real dynamics is dissipative but we have only to consider the reversible part in calculating the equal-time correlation at the equilibrium. As discussed in Ref. 28, we think that our results can be checked experimentally by means of the membrane with the inverted polarity in some organic binary mixture, for example.

The following assumptions are shared by Ref. 28 and this study. The temperature is homogeneous and constant. The membrane is made up of a single component, immersed in an incompressible binary fluid mixture, and regarded as a thin film fluctuating around a plane. The mixture has the same properties on both sides of the membrane. Far from the membrane, it is static and in the homogeneous phase near the demixing critical point. The preferential attraction comes from a short-ranged interaction and is represented by the surface field. Our calculation is performed within the linear approximation with respect to the undulation amplitude; the equilibrium state for the flat membrane is the reference state *or* unperturbed state. We describe our formulation in Sec. II and improve the previous calculation procedure in Sec. III. It is shown in Sec. IV A that, if the same assumptions are imposed, the improved procedure yields the same result as that of Ref. 28. In Sec. IV B, we use the improved procedure to calculate the means square amplitude in the Gaussian model without assuming the surface field to be weak.

In the results of the Gaussian model, the restoring force becomes larger with the correlation length far from the membrane, as is shown later by Eqs. (52) and (67). It is of interest to examine whether this tendency remains when this correlation length becomes sufficiently long in the mixture very close to critical point. Then, the mixture takes the universal properties around the normal transition mentioned below. In the three-dimensional Ising model in a finite lattice in the absence of bulk and surface fields, if the coupling between neighboring spins at the surface regions is much stronger than that of the

bulk, the extraordinary second-order transition occurs in the bulk in the presence of spontaneously ordered surface [29–33]. This transition shares the universal properties with the normal transition, where the surface has been ordered by a surface field imposed externally. The normal transition is exhibited by a binary fluid mixture filled in a container when the preferential attraction is caused by a short-ranged interaction. This situation is totally the same as the one considered in the unperturbed state here. The critical adsorption occurs in the mixture in a semi-infinite region bounded by a flat wall [17–20, 34]. The order parameter profile has universal properties around the critical point whether it is in the one-phase region or in the two-phase region [33, 35–37]. Mainly in the latter region, the wetting phenomenon is involved [30, 38, 39]. In the previous renormalization group theory for the extraordinary transition, the order parameter is coarse-grained and rescaled. According to the mapping between extraordinary and normal transitions, the surface field appears to diverge at the normal transition [33, 40].

In Sec. V, we assume the critical fraction far from the membrane and consider the undulation by using the renormalized local functional theory, which is proposed by Okamoto and Onuki [21]. They study the universal properties of a near-critical mixture intercalated by two parallel walls and the adsorption-induced interaction, and elucidate the phase transition of the capillary condensation. The interaction between two spheres is also studied [41]. In these studies, the order-parameter is taken to be sufficiently large at the interface between the mixture and wall for convenience. This appears in harmony with the divergence of the surface field mentioned in the preceding paragraph. However, we should do without this convenience because the order parameter is not rescaled in the renormalized local functional theory. This problem is crucial not only because it involves the boundary condition but also because it affects our hydrodynamic formulation and perturbation scheme. We calculate interfacial properties of the unperturbed profile by using a fixed surface field in Sec. V A, and show that the results are consistent with the previous results on the normal transition in Sec. V B. Thus, we can assume a finite surface field to study the undulation by using the renormalized local functional theory. The results in this framework are shown in Sec. V C. Section VI gives the summary and outlook of this study. The numerical results in this study are obtained with the aid of Mathematica (Wolfram Research).

II. FORMULATION

The mass-density difference between the two components, denoted by φ , depends on the position \mathbf{r} in the binary mixture. Near the critical point, the φ -dependent part of the free-energy functional for the mixture bulk is

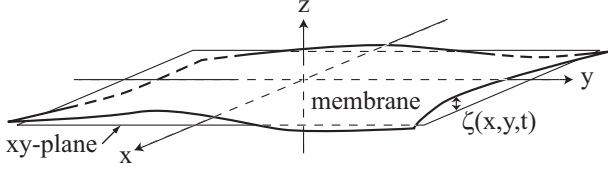


FIG. 1: A fluid membrane made up of a single component fluctuates around the xy plane. The ambient mixture has the same properties on both sides of the membrane.

assumed to be of the Ginzburg-Landau type [42]. The preferential attraction due to some short-ranged interaction is represented by the potential f_s determined by the value of φ immediately near the membrane [39]. Thus, the φ -dependent part of the free-energy functional is given by

$$\int_{C^e} d\mathbf{r} \left\{ f(\varphi(\mathbf{r})) + \frac{1}{2} M |\nabla\varphi(\mathbf{r})|^2 \right\} + \int_{\partial C} dS f_s(\varphi(\mathbf{r})) . \quad (1)$$

The first integral is the volume integral over the regions on both sides of the membrane (C^e), where the mixture lies, and f is a function of φ . The coefficient M is a positive function of φ in general. The second integral is the surface integral over the interfaces on both sides of the membrane (∂C). We assume f_s to be a linear function; $-df_s(\varphi)/(d\varphi) = h$ is called surface field. Equation (1) is a result of coarse graining and is renormalized up to the local correlation length. If the mixture is near but not very close to the critical point, the correlation length is so short that f and M can be regarded as a quadratic function and a constant, respectively. Then, we have the Gaussian model, which is considered in Sec. IV. General cases are considered in Sec. V.

As stated in the third paragraph of Sec. I, we utilize the hydrodynamics in the limit of no dissipation. The hydrodynamics derived from the bulk part of Eq. (1) is well known in the model H, a standard model for near-critical fluid dynamics [42, 43]. Dependence of φ on the time t is thus considered below. The Cartesian coordinate system (x, y, z) is set so that the membrane fluctuates around the xy -plane (Fig. 1). The unit vectors along the coordinate axes are denoted by $\mathbf{e}_x, \mathbf{e}_y$, and \mathbf{e}_z , respectively. The z coordinate of the membrane is referred to as ζ , which is a function of x, y , and t .

The chemical potential conjugate to φ is given by

$$\mu(\mathbf{r}, t) = f'(\varphi(\mathbf{r}, t)) - \frac{1}{2} M' |\nabla\varphi|^2 - M \Delta\varphi(\mathbf{r}, t) . \quad (2)$$

Hereafter, the prime indicates the derivative with respect to the variable, *e.g.*, $f' = df/(d\varphi)$ and $M' = dM/(d\varphi)$, while the double prime means the second derivative. We

write \mathbf{n} for the unit vector which is normal to the membrane and is directed towards the positive- z side. The local equilibrium at the interface gives the boundary condition [27]

$$\pm M \mathbf{n} \cdot \nabla\varphi = -h \quad \text{as } z \rightarrow \zeta \pm , \quad (3)$$

where $z \rightarrow \zeta + (-)$ means that z approaches $\zeta(x, y, t)$ with $z - \zeta > 0$ (< 0) maintained. The reversible part of the pressure tensor is given by

$$\Pi = \left(p - f + \mu\varphi - \frac{M}{2} |\nabla\varphi|^2 \right) \mathbf{1} + M \nabla\varphi \nabla\varphi , \quad (4)$$

where $\mathbf{1}$ denotes the isotropic tensor. The scalar p comes from the dependence of the free-energy functional on the mass density of the mixture ρ . We write \mathbf{V} for the velocity field in the mixture. Assuming ρ to be a constant as in the previous works [4, 48–50], we have

$$\nabla \cdot \mathbf{V} = 0 . \quad (5)$$

We thus regard p as dependent on \mathbf{r} and t irrespective of the local state. We need not assume viscosity to calculate the equal-time correlation. Because $\nabla \cdot \Pi$ equals $\nabla p + \varphi \nabla\mu$, the dynamics of the mixture follows

$$\rho \frac{\partial \mathbf{V}}{\partial t} = -\nabla p - \varphi \nabla\mu , \quad (6)$$

where the convective term is neglected in anticipation of the later linear approximation. The limit of zero viscosity in the hydrodynamics of the mixture causes the well-known boundary layer problem of the velocity field. Using the slip boundary condition on each side of the membrane, we deal with steep changes in the tangential velocity components within the thin boundary layers immediately near the membrane [44]. We below consider only outside these boundary layers; the tangential components of the velocity need not be continuous across the membrane, while the normal component is continuous.

Far from the membrane, the mixture is assumed to be static and in the homogeneous phase, *i.e.*, \mathbf{V} vanishes and φ is constant. There, μ and p are also constant, considering Eqs. (2) and (6). The constant values of φ , μ , and p are respectively denoted by φ_∞ , $\mu^{(0)} \equiv f'(\varphi_\infty)$, and $p^{(0)}$, which are shared by the mixture regions on both sides of the membrane. Considering that the static pressure far from the membrane is given by $p^{(0)} - f(\varphi_\infty) + \mu^{(0)}\varphi_\infty$ because of Eq. (4), adding a linear function of φ to f does not change the dynamics; Eq. (6) remains unchanged if constants are added to $p^{(0)}$ and $\mu^{(0)}$. This point is to be noted in Sec. V C. The stress exerted on the membrane by the mixture on the positive- z (negative- z) side is denoted by $\mathbf{F}^{(+)} (\mathbf{F}^{(-)})$. We define the mean curvature of the membrane H so that its sign is positive when the center of curvature lies on the side towards which \mathbf{n} is directed. We have

$$\mathbf{F}^{(\pm)} = \lim_{z \rightarrow \zeta \pm} \{ \mp \Pi \cdot \mathbf{n} + \nabla_{\parallel} f_s + 2H f_s \mathbf{n} \} , \quad (7)$$

where ∇_{\parallel} implies the projection of ∇ on the tangent plane [45]. The last two terms above come from the stress due to the two-dimensional pressure $-f_s$, and we use Eq. (3) to find that the tangential components of $\mathbf{F}^{(\pm)}$ vanishes, as discussed in Appendices A and D of Ref. 25.

In the previous works [23–27], the diffusive flux between the two components is considered. Because it is proportional to the gradient of μ , the mass conservation of each component leads to

$$\frac{\partial \varphi}{\partial t} = -\mathbf{V} \cdot \nabla \varphi + \nabla \cdot L \nabla \mu , \quad (8)$$

where the Onsager coefficient L is a positive function of φ . Assuming that the diffusion flux cannot pass across the membrane leads to

$$\mathbf{n} \cdot L \nabla \mu = 0 \quad \text{as } z \rightarrow \zeta \pm . \quad (9)$$

The diffusion should not be involved in the equal-time correlation considered here, and we will take the limit of $L \rightarrow 0+$ at and after Eq. (32) below. Still, we use these two equations at this stage because this limit gives rise to another boundary layer problem; L is associated with the highest-order derivative in Eq. (8) and the limit of $L \rightarrow 0+$ involves the singular perturbation. The same procedure is used in Ref. 28.

Our calculation is performed within the linear approximation with respect to the undulation amplitude. Introducing a dimensionless parameter ε , we define nonzero $\zeta^{(1)}$ so that we have

$$\zeta(\mathbf{x}, t) = \varepsilon \zeta^{(1)}(\mathbf{x}, t) , \quad (10)$$

where \mathbf{x} represents a position on the membrane and has coordinates (x, y) . Assuming the spontaneous curvature to vanish, we write $c_b H^2$ for the bending energy per unit area of the membrane, where c_b is the bending rigidity [1, 2]. The restoring force is normal to the membrane, and its component along \mathbf{n} is given by [46, 47]

$$F_r = -c_b \left(\frac{\partial^2}{\partial x^2} + \frac{\partial^2}{\partial y^2} \right) H . \quad (11)$$

Let us write $\mathbf{v}(\mathbf{x}, t)$ for the velocity field of the membrane. Assuming the membrane to be compressible, we write $\rho_m(\mathbf{x}, t)$ for the membrane mass per unit area, and $p_m(\mathbf{x}, t)$ for its in-plane pressure field. In contrast with f_s , p_m does not depend explicitly on the value of φ immediately near the membrane. Neglecting the membrane viscosity, we can write the mass conservation and momentum conservation of the membrane [48–51]. Up to

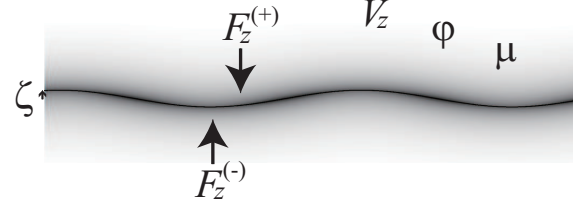


FIG. 2: A cross section, along the z -axis, of a fluctuating membrane (solid curve) is schematically drawn. The gray scale represents the adsorption layer. At the order of ε , the z -component of the stress exerted on the membrane, $F_z = F_z^{(+)} + F_z^{(-)}$, is calculated from the fields of the mixture, V_z , φ , and μ . They are changed by the membrane motion, which is represented by the change of ζ . We nondimensionalize their Fourier transforms at this order, $\tilde{V}_z^{(1)}$, $\tilde{\varphi}^{(1)}$, and $\tilde{\mu}^{(1)}$, to introduce U , G , and Q at Eqs. (23)–(25), respectively.

the order of ε , the tangential motion is independent of the normal motion, which is represented by

$$\rho_m \frac{\partial v_z}{\partial t} = F_z + F_r - 2H p_m . \quad (12)$$

Here, $F_z \equiv F_z^{(+)} + F_z^{(-)}$ denotes the z -component of the total stress exerted by the mixture. To obtain the restoring force due to the ambient near-criticality, we should analyze the fields of the mixture to elucidate what stress F_z is exerted when the membrane height is given by ζ (Fig. 2).

III. EXPANSIONS WITH RESPECT TO THE FLUCTUATION AMPLITUDE

The membrane is fixed on the xy -plane in the unperturbed state ($\varepsilon = 0$), where μ is homogeneous and so is p because of Eq. (6) [27]. They are respectively given by the constants $\mu^{(0)}$ and $p^{(0)}$. Up to the order of ε , we expand the fields as

$$\begin{aligned} \varphi(\mathbf{r}, t) &= \varphi^{(0)}(z) + \varepsilon \varphi^{(1)}(\mathbf{r}, t) , \\ \mu(\mathbf{r}, t) &= \mu^{(0)} + \varepsilon \mu^{(1)}(\mathbf{r}, t) , \\ p(\mathbf{r}, t) &= p^{(0)} + \varepsilon p^{(1)}(\mathbf{r}, t) , \\ \text{and } \mathbf{V}(\mathbf{r}, t) &= \varepsilon \mathbf{V}^{(1)}(\mathbf{r}, t) . \end{aligned} \quad (13)$$

The field with the superscript (0) is defined so that it is independent of ε , while the field with the superscript (1) is defined so that it becomes proportional to ε after being multiplied by ε . The fields with the superscript (1) in Eq. (13) vanish far from the membrane. As shown below, the fields $V_z^{(1)}$, $\varphi^{(1)}$, and $\mu^{(1)}$ satisfy a set of simultaneous equations, Eqs. (16), (A3), and (A4).

Because of the symmetry of the unperturbed state, $\varphi^{(0)}$ depends only on z and is even with respect to

z . We write M_0 , M'_0 , and M''_0 for $M(\varphi^{(0)})$, $M'(\varphi^{(0)})$, and $M''(\varphi^{(0)})$, respectively. The prime indicates the derivative, as stated below Eq. (2). We write M_{00} for $M(\varphi^{(0)}(0+))$, which is $M(\varphi^{(0)}(z))$ in the limit of $z \rightarrow 0+$ and is a constant unlike M_0 . As argued for a mixture in contact with a flat wall [39], Eq. (2) yields

$$f'(\varphi^{(0)}) - M_0 \varphi^{(0)''} - \frac{M'_0}{2} \left| \varphi^{(0)'} \right|^2 = \mu^{(0)} , \quad (14)$$

while Eq. (3) yields

$$M_{00} \frac{\partial}{\partial z} \varphi^{(0)} = \mp h \quad \text{as } z \rightarrow 0 \pm . \quad (15)$$

Using Eqs. (14) and (15), if h vanishes, we find $\varphi^{(0)}$ equal to φ_∞ over the mixture. Equations (14) and (15) are available not only in the Gaussian model but in genral as far as Eq. (1) is renormalized up to the local correlation length, as is discussed in Sec. V.

Let us consider the terms at the order of ε . From Eq. (2), we have

$$\left\{ M_0 \Delta + M'_0 \varphi^{(0)'} \frac{\partial}{\partial z} + N(z) \right\} \varphi^{(1)} = -\mu^{(1)} , \quad (16)$$

where the definition of $N(z)$ is relegated to Eq. (A1). The boundary condition, Eq. (3), should hold in both the unperturbed and perturbed states. Thus, from Eqs. (3) and (15), as $z \rightarrow 0 \pm$ we have

$$\frac{\partial \varphi^{(1)}}{\partial z} + \varphi^{(0)''} \zeta^{(1)} = -\frac{h M'_0}{M_0^2} \left(\frac{h \zeta^{(1)}}{M_0} \mp \varphi^{(1)} \right) , \quad (17)$$

which becomes Eq. (29) of Ref. 28 if M is a constant. Even otherwise, the right-hand side (rhs) above vanishes in the limit of $L \rightarrow 0+$, as shown later. The slip boundary condition gives

$$\lim_{z \rightarrow 0 \pm} V_z^{(1)} = v_z^{(1)} = \frac{\partial \zeta^{(1)}}{\partial t} . \quad (18)$$

Equation (9) leads to

$$L \frac{\partial \mu^{(1)}}{\partial z} \rightarrow 0 \quad \text{as } z \rightarrow 0 \pm . \quad (19)$$

We write (\mathbf{x}, z) for $\mathbf{r} = (x, y, z)$. In the directions of x and y , we impose the periodic boundary condition and add an overhat to the Fourier transform, e.g.,

$$\hat{p}^{(1)}(\mathbf{k}, z, t) \equiv \frac{1}{l_p^2} \int_0^{l_p} dx \int_0^{l_p} dy p^{(1)}(\mathbf{x}, z, t) e^{-i\mathbf{k} \cdot \mathbf{x}} , \quad (20)$$

where \mathbf{k} represents (k_x, k_y) with $l_p k_x / (2\pi)$ and $l_p k_y / (2\pi)$ being integers. The period l_p should be sufficiently large as compared with the relevant correlation length, and can be regarded as representing the membrane size. We add

an overtilde to the further Fourier transform with respect to t , e.g.,

$$\tilde{p}^{(1)}(\mathbf{k}, z, \omega) = \frac{1}{2\pi} \int_{-\infty}^{\infty} dt \hat{p}^{(1)}(\mathbf{k}, z, t) e^{i\omega t} . \quad (21)$$

Using a length ξ_a , which is later defined suitably, we introduce a dimensionless parameter

$$\lambda \equiv \frac{\sqrt{M_{00} \xi_a^{5/2}}}{\sqrt{c_b}} \varphi^{(0)''}(0+) , \quad (22)$$

which vanishes if h vanishes because $\varphi^{(0)''}(0+)$ then vanishes for the reason stated below Eq. (15). Using $Z \equiv z/\xi_a$, we introduce a dimensionless field

$$U(\mathbf{k}, Z, \omega) \equiv \frac{i \tilde{V}_z^{(1)}(\mathbf{k}, z, \omega)}{\omega \tilde{\zeta}^{(1)}(\mathbf{k}, \omega)} . \quad (23)$$

Judging from Eqs. (16), (17), (19), and (A4), $\varphi^{(1)}$ and $\mu^{(1)}$ vanish if h vanishes. Thus, we introduce dimensionless fields

$$G(\mathbf{k}, Z, \omega) \equiv \frac{\tilde{\varphi}^{(1)}(\mathbf{k}, z, \omega)}{\xi_a \varphi^{(0)''}(0+) \tilde{\zeta}^{(1)}(\mathbf{k}, \omega)} \quad (24)$$

and

$$Q(\mathbf{k}, Z, \omega) \equiv \frac{\xi_a \tilde{\mu}^{(1)}(\mathbf{k}, z, \omega)}{M_{00} \varphi^{(0)''}(0+) \tilde{\zeta}^{(1)}(\mathbf{k}, \omega)} . \quad (25)$$

Below, we sometimes write $U(Z)$ for $U(\mathbf{k}, Z, \omega)$, and also use this kind of conciseness for G , Q , and their outer solutions introduced below. Writing k for $|\mathbf{k}|$, we define K as $k \xi_a$. It is convenient to introduce

$$\Xi(Z) \equiv \frac{\varphi^{(0)'}(z)}{\xi_a \varphi^{(0)''}(0+)} \quad (26)$$

and

$$\Lambda \equiv \frac{K \varphi^{(0)''}(0+) \sqrt{M_{00}}}{\omega \sqrt{\rho}} = \lambda \frac{k \sqrt{c_b}}{\omega \sqrt{\rho \xi_a^3}} . \quad (27)$$

From the x - and y -components of the Fourier transforms of Eq. (6), we use Eq. (5) to obtain Eq. (A3), which leads to

$$(\partial_Z^2 - K^2) U(Z) = \Lambda^2 \Xi(Z) Q(Z) \quad (28)$$

for $\pm Z > 0$. Hereafter, ∂_Z implies the partial derivative with respect to Z and ∂_Z^2 denotes $\partial_Z \partial_Z$. We have $U \rightarrow 1$ as $Z \rightarrow 0+$ because of Eqs. (18) and (23), while $U \rightarrow 0$ as $Z \rightarrow \infty$ as stated below Eq. (13). Applying the method of variation of parameters to Eq. (28), we obtain for $Z > 0$

$$U(Z) = \left\{ 1 + \frac{\Lambda^2}{2K} \int_0^\infty dZ_1 Q(Z_1) \Xi(Z_1) e^{-K Z_1} \right\} e^{-K Z} + \Lambda^2 \int_0^\infty dZ_1 \Gamma_K(Z, Z_1) Q(Z_1) \Xi(Z_1) , \quad (29)$$

where the kernel is defined as

$$\Gamma_K(Z, Z_1) = -\frac{1}{2K} e^{-K|Z-Z_1|} \quad (30)$$

for $Z > 0$ and $Z_1 > 0$ [28]. From Eq. (29), up to the order of Λ , we have

$$U(Z) = e^{-KZ} \quad (31)$$

for $Z > 0$ irrespective of the boundary layer of the chemical potential mentioned below Eq. (9).

Picking up the terms at the order of ε of Eq. (8), we have Eq. (A4), whose naive limit of $L \rightarrow 0+$ leads to contradiction among the boundary conditions if h does not vanish, as discussed below Eq. (A4). Its naive limit gives a relation between the outer solutions, *i.e.*, the solutions outside the boundary layer [52]. Below, the subscript _{out} indicates the outer solution. For example, $\tilde{\varphi}_{\text{out}}^{(1)}$ denotes the outer solution of $\tilde{\varphi}^{(1)}$, and G_{out} is defined as the rhs of Eq. (24) with $\tilde{\varphi}^{(1)}$ being replaced by $\tilde{\varphi}_{\text{out}}^{(1)}$. The relation between the outer solutions mentioned above is $i\omega\tilde{\varphi}_{\text{out}}^{(1)} = \varphi^{(0)'}\tilde{V}_{z\text{out}}^{(1)}$, which is rewritten as

$$G_{\text{out}}(\mathbf{k}, Z, \omega) = -\Xi(Z)U_{\text{out}}(\mathbf{k}, Z, \omega). \quad (32)$$

Replacing $\varphi^{(1)}$ and $\mu^{(1)}$ by their respective outer solutions in Eq. (16), we use Eq. (32) to obtain

$$Q_{\text{out}} = \frac{M_0\Xi}{M_{00}}(\partial_Z^2 - K^2)U_{\text{out}} + \frac{1}{M_{00}\Xi} \frac{\partial U_{\text{out}}}{\partial Z} \frac{dM_0\Xi^2}{dZ}, \quad (33)$$

where we utilize the fact that the rhs of Eq. (16) vanishes when $\varphi^{(1)}$ is replaced by $\varphi^{(0)'}$ on the left-hand side (lhs). This is verified by differentiating Eq. (14) with respect to z .

In the limit of $L \rightarrow 0+$, Q_{out} is defined for $Z > 0$. Subtracting Q_{out} in this limit from Q , we define Q_{in} as the difference, which cannot be neglected in the integrals of Eq. (29) even in the limit of $L \rightarrow 0+$. Assuming that $Z(> 0)$ lies outside the boundary layer in Eq. (29), we find $U_{\text{out}}(Z)$ independent of Q_{in} to obtain

$$\lim_{Z \rightarrow 0+} \partial_Z U_{\text{out}} = -K - \Lambda^2 \int_0^\infty dZ_1 Q_{\text{out}}(Z_1) \Xi(Z_1) e^{-KZ_1} \quad (34)$$

in the limit of $L \rightarrow 0+$. In this limit, Eq. (29) also yields

$$\lim_{Z \rightarrow 0+} \partial_Z U = \lim_{Z \rightarrow 0+} \partial_Z U_{\text{out}} - \Lambda^2 \Xi(0+) \int_0^\infty dZ_1 Q_{\text{in}}(Z_1), \quad (35)$$

which contains the integral of Q_{in} . In Eq. (41) below, the Fourier transform of the stress exerted on the membrane involves Eq. (35).

As discussed above Eq. (A5), considering the Fourier transforms of Eqs. (16) and (17), $\tilde{\mu}^{(1)}$ and $\partial^2 \tilde{\varphi}^{(1)}/(\partial z^2)$ behave like the delta function diverging at the interface.

We integrate Eq. (16) over the boundary layer to obtain Eq. (A5), which leads to

$$\lim_{Z \rightarrow 0+} (\partial_Z G_{\text{out}} - \partial_Z G) = - \int_0^\infty dZ Q_{\text{in}}(Z) \quad (36)$$

in the limit of $L \rightarrow 0+$. In this limit, we find

$$\lim_{Z \rightarrow 0+} U_{\text{out}} = 1 \quad (37)$$

from Eqs. (18) and (A6), and

$$\lim_{Z \rightarrow 0\pm} \partial_Z G = -1 \quad (38)$$

from Eqs. (17) and (A7). Differentiating Eq. (32) with respect to Z and taking the limit of $Z \rightarrow 0+$, we obtain

$$\lim_{Z \rightarrow 0+} \partial_Z G_{\text{out}} = -\Xi(0+) \lim_{Z \rightarrow 0+} \partial_Z U_{\text{out}} - 1 \quad (39)$$

because of $\Xi'(0+) = 1$. Noting that the rhs of Eq. (36) equals that of Eq. (39), we can delete the integral of Q_{in} from Eq. (35) to obtain

$$\lim_{Z \rightarrow 0+} \partial_Z U = \{1 - \Lambda^2 \Xi(0+)^2\} \lim_{Z \rightarrow 0+} \partial_Z U_{\text{out}}. \quad (40)$$

We define $F_z^{(1)}$ so that $\varepsilon F_z^{(1)}$ equals F_z up to the order of ε . In Eq. (7), we use Eqs. (3), (14), (23), (38), (A2), and (A7) to obtain

$$\tilde{F}_z^{(1)} = -2k^2 \tilde{\zeta}^{(1)} f_s(\varphi^{(0)}(0+)) - \frac{2\rho\omega^2 \tilde{\zeta}^{(1)}}{\xi_a k^2} \lim_{Z \rightarrow 0+} \partial_Z U, \quad (41)$$

where we note that \tilde{H} equals $-\varepsilon k^2 \tilde{\zeta}^{(1)}/2$ and that $\tilde{V}_z^{(1)}$ is even with respect to z . Equation (41) is also used in Ref. 28 [53]. Like Eq. (13), we expand the membranous fields; we write $\rho_m^{(0)}$ and $p_m^{(0)}$ for the constant terms of ρ_m and p_m independent of ε , respectively. Equations (11), (12), and (18) yield

$$-\rho_m^{(0)} \omega^2 \tilde{\zeta}^{(1)} = \tilde{F}_z^{(1)} - \left(\frac{c_b k^4}{2} - p_m^{(0)} k^2 \right) \tilde{\zeta}^{(1)}, \quad (42)$$

which describes the membrane undulation. Into this equation, we can substitute Eq. (41); we have only to consider the outer solutions in the limit of $L \rightarrow 0+$ because of Eq. (40). The mean lateral tension, mentioned in the first paragraph of Sec. I, is given by the negative of the equilibrium average of the membrane pressure, $-p_m^{(0)}$, when the preferential attraction does not work. When it works, as stated below Eq. (7), we should take into account the two-dimensional pressure $-f_s$ on each side of the membrane. Thus, in general, we should regard

$$\sigma_1 \equiv -p_m^{(0)} + 2f_s(\varphi^{(0)}(0+)) \quad (43)$$

as the mean lateral tension, which vanishes when the membrane is suspended freely in a near-critical binary fluid mixture [28].

IV. GAUSSIAN MODEL

In this section, we assume the Gaussian model, where M is a positive constant and $f(\varphi)$ is given by

$$\frac{m}{2}(\varphi - \varphi_\infty)^2 + \mu^{(0)}(\varphi - \varphi_\infty), \quad (44)$$

with m being defined as a positive constant. Using Eq. (44) in Eq. (1) amounts to assuming that the mixture is near, but not very close to, the demixing critical point [42]. In the Gaussian model, $\xi_c \equiv \sqrt{M/m}$ gives the correlation length far from the membrane. From Eqs. (14) and (15), we have

$$\varphi^{(0)}(z) = \varphi_\infty + \frac{h\xi_c}{M}e^{-|z|/\xi_c}, \quad (45)$$

which is the same as Eq. (27) of Ref. 28. This is essentially calculated in Ref. 39 and is also found in Sec. IIA of Ref. 30. Below, as for the mixture, we consider only the fields on the side of $z > 0$; the fields on the other side need not be considered in Eq. (41).

Let us put ξ_a equal to ξ_c in the Gaussian model. Accordingly, we have $Z = z/\xi_c$ and $K = k\xi_c$, which are respectively the dimensionless z -coordinate and wavenumber introduced above Eqs. (23) and (26). We use Eq. (26) to find

$$\Xi(Z) = -e^{-Z}, \quad (46)$$

where we assume $Z > 0$ as stated above. From Eqs. (22), (27), and (45), we here have

$$\lambda^2 = \frac{h^2\xi_c^3}{c_b M} \quad \text{and} \quad \Lambda^2 = \frac{h^2 k^2}{M\rho\omega^2}. \quad (47)$$

A. The previous result for the weak preferential attraction

For a sufficiently small surface field, we can assume λ^2 to be so small that $\Lambda^2 \ll 1$ holds for the values of k and ω to be considered in a membrane with a given size. On this assumption, the mean square amplitude is calculated in Ref. 28, where the condition for the membrane size is not fully discussed. The condition is discussed in the next subsection. The procedure used in Ref. 28 is as follows. Substituting Eq. (31) into Eq. (33) yields Q_{out} up to the order of Λ . Because the Gaussian model Eq. (44) is assumed, we can solve Eq. (16) to express G in terms of Q by using the method of variation of parameters. This result yields G_{out} , which is required to be consistent with Eq. (32) into which Eq. (31) is substituted. From this requirement, we can obtain the last term on the rhs of Eq. (35), which is used in rewriting the second term on the rhs of Eq. (41). When h is positive, $\varphi(\mathbf{x}, \zeta+, t)$ is larger (smaller) than

$\varphi(\mathbf{x}, \zeta-, t)$ for $\zeta > 0$ ($\zeta < 0$) within this approximation.

In the present study, we can improve the procedure to the previous result as follows because Eq. (40) is derived from Eq. (36) representing the interfacial property of Eq. (16). We use Eq. (31) in Eq. (33) to obtain Q_{out} up to the order of Λ . Substituting this result into Eq. (34), we obtain

$$\lim_{Z \rightarrow 0+} \partial_Z U_{\text{out}} = -K - \Lambda^2 K + \Lambda^2 d_0(K) \quad (48)$$

up to the order of Λ^3 , where we use

$$d_0(K) \equiv \frac{K^2}{K+1}. \quad (49)$$

We substitute Eq. (48) into Eq. (40) to obtain

$$\lim_{Z \rightarrow 0+} \partial_Z U = -K + \Lambda^2 d_0(K) \quad (50)$$

up to the order of Λ^3 . Up to the same order, substituting Eq. (50) into Eq. (41), we rewrite Eq. (42) as

$$\rho_k^{(\text{eff})} \omega^2 \tilde{\zeta}^{(1)} = \left\{ \frac{c_b}{\xi_c^4} \left(\frac{K^4}{2} + 2\lambda^2 d_0(K) \right) \right\} \tilde{\zeta}^{(1)} \quad (51)$$

for a tensionless membrane, with the aid of the second equality of Eq. (27). We use $\rho_k^{(\text{eff})} \equiv \rho_m^{(0)} + 2\rho/k$, whose second term represents the induced-mass density. Suppose that a value of k is given. Then, if the assumption $\Lambda^2 \ll 1$ is valid for any ω to be considered, Eq. (51) can be inversely Fourier-transformed to give

$$\rho_k^{(\text{eff})} \frac{\partial^2}{\partial t^2} \hat{\zeta}^{(1)} = - \left\{ \frac{c_b}{\xi_c^4} \left(\frac{K^4}{2} + 2\lambda^2 d_0(K) \right) \right\} \hat{\zeta}^{(1)}. \quad (52)$$

This represents the small oscillation about the equilibrium point, and thus its potential energy can be found. The correlation length ξ_c is relevant in this result; $K = k\xi_c \ll 1$ should be required for our hydrodynamic formulation to be valid because it is based on a coarse-grained free-energy functional, Eq. (1). Thus, the first term is much larger than the second term in the parentheses above when $K^2 \gg 4\lambda^2$ holds, considering $d_0(K) \approx K^2$. As stated later, when the Gaussian model is valid, ξ_c is typically several nanometers. For this value, any practical membrane can have modes with $K \equiv k\xi_c \ll 1$.

Using the equipartition theorem, we obtain the mean square amplitude for each wavenumber mode. For a tensionless membrane, if Eq. (52) is valid, we obtain

$$\begin{aligned} & \langle \hat{\zeta}(\mathbf{k}, t) \hat{\zeta}(\mathbf{k}', t) \rangle \\ &= \delta_{\mathbf{k}, -\mathbf{k}'} \frac{k_B T}{l_p^2} \left\{ \frac{c_b k^4}{2} + \frac{2h^2}{M\xi_c} d_0(k\xi_c) \right\}^{-1}, \end{aligned} \quad (53)$$

where $\langle \cdots \rangle$ indicates the equilibrium average at the temperature T and k_B denotes the Boltzmann constant.

The temperature T can be replaced approximately by the critical temperature, denoted by T_c . The term in the brackets of Eq. (52) is the same as the sum in the brackets of Eq. (53). If $\sigma_1 k^2$ is supplemented, these results are respectively the same as Eqs. (73) and (75) of Ref. 28, where $\sigma_1 = 0$ is not assumed. The ambient near-criticality represented by the second term in the brackets of Eq. (53) tends to suppress the mean square amplitude; this term is approximately equal to $2h^2 k^2 \xi_c / M$ for $k\xi_c \ll 1$.

Equation (40) makes it unnecessary to solve Eq. (16) explicitly and enables us to calculate Eq. (41) directly from the outer solution U_{out} . We can derive a closed equation for U_{out} without assuming $\Lambda^2 \ll 1$; it is given by Eq. (57) below and is solved in the Gaussian model. We also apply Eq. (40) to the non-Gaussian model, as discussed in Sec. V C.

B. Arbitrary magnitude of the preferential attraction

Terms with the higher orders with respect to Λ are neglected in Eqs. (48) and (50). When h does not vanish, we define d_1 so that the lhs exactly equals the rhs in Eq. (50) with d_0 being replaced by $d_0(1 + d_1)$, *i.e.*,

$$d_1 \equiv \frac{\lim_{Z \rightarrow 0+} \partial_Z U + K}{\Lambda^2 d_0(K)} - 1. \quad (54)$$

We do not suppose $k = 0$ because this mode represents not the undulation but the translational shift without the restoring force. Thus, the denominator in Eq. (54) does not vanish. For a tensionless membrane, we can rewrite Eq. (42) as

$$\rho_k^{(\text{eff})} \omega^2 \tilde{\zeta}^{(1)} = \left\{ \frac{c_b k^4}{2} + \frac{2h^2}{M\xi_c} d_0 (1 + d_1) \right\} \tilde{\zeta}^{(1)} \quad (55)$$

with all the higher terms of Λ contained. As shown later, more than one frequency allows $\tilde{\zeta}^{(1)} \neq 0$ for a small value of K , and thus $\hat{\zeta}$ is not always a normal mode.

Substituting Eq. (45) into Eq. (33) yields

$$Q_{\text{out}} = \{-e^{-Z} (\partial_Z^2 - K^2) + 2e^{-Z} \partial_Z\} U_{\text{out}}. \quad (56)$$

Thus, with the aid of Eq. (28), we obtain

$$(1 - \Lambda^{-2} e^{2Z}) (\partial_Z^2 - K^2) U_{\text{out}} = 2\partial_Z U_{\text{out}}. \quad (57)$$

The boundary conditions are given by Eq. (37) and $U_{\text{out}} \rightarrow 0$ as $Z \rightarrow \infty$. Let us introduce $\mathcal{U}_o(\theta)$ so that we have

$$U_{\text{out}}(\mathbf{k}, Z, \omega) = e^{(1-K_1)Z} \mathcal{U}_o(\theta), \quad (58)$$

where $\theta(>0)$ is defined as $\Lambda^{-2} e^{2Z}$ and K_1 is defined as $\sqrt{1 + K^2}$. Introducing

$$a \equiv \frac{1}{2}(1 - K - K_1) \quad \text{and} \quad b \equiv \frac{1}{2}(1 + K - K_1), \quad (59)$$

we rewrite Eq. (57) as

$$\theta(1 - \theta) \mathcal{U}_o'' + \{a + b - (a + b + 1)\theta\} \mathcal{U}_o' - ab \mathcal{U}_o = 0, \quad (60)$$

which is Gauss' differential equation [55, 56].

The governing equations and the boundary conditions in Sec. II determine the fields of the mixture uniquely. Thus, Eq. (57) in the limit of $L \rightarrow 0+$ determines U_{out} uniquely with the aid of the boundary conditions at $Z \rightarrow 0+$ and ∞ . Because $V_z^{(1)}$ is real, we use Eq. (23) to find $U_{\text{out}}(\mathbf{k}, Z, \omega)$ and $U_{\text{out}}(-\mathbf{k}, Z, -\omega)$ are complex conjugates of each other. They should be identical as the unique solution of Eq. (57), and thus U_{out} is real although U can have an imaginary part within the boundary layer. This means that the phase difference between the nondissipative oscillations of $\hat{\zeta}$ and $\hat{V}_{z \text{ out}}^{(1)}$ is π , considering Eq. (23). We find the solution to be given by $\mathcal{U}_o(\theta) = g(\theta)/g(\Lambda^{-2})$, where g is defined as

$$g(\theta) \equiv \begin{cases} \theta^{-b} \mathcal{F}(1 - a, b, 1 + b - a, \theta^{-1}) & \text{for } \theta > 1 \\ \{f_0^+(\theta) + f_0^-(\theta)\} / 2 & \text{for } 0 < \theta < 1 \end{cases}. \quad (61)$$

Here, \mathcal{F} denotes Gauss' hypergeometric series, while each of f_0^\pm is a linear combination of hypergeometric series defined by Eq. (B2). The difference in the first parentheses on the lhs of Eq. (57) vanishes at $\theta = 1$, which suggests some singularity of the solution. In fact, as shown in Appendix B, $g(\theta)$ diverges logarithmically at $\theta = 1$. Because the divergence is logarithmic, however, $\hat{V}_{\text{out}}^{(1)}(\mathbf{k}, Z, t)$ does not diverge. Using

$$\lim_{Z \rightarrow 0+} \partial_Z U_{\text{out}} + K = 2 \left\{ b + \frac{g'(\Lambda^{-2})}{\Lambda^2 g(\Lambda^{-2})} \right\}, \quad (62)$$

we can calculate d_1 with the aid of Eqs. (40), (46), and (54). Because Eq. (62) is real, the sum in the brackets of Eq. (55) is real, as it should be because Eq. (55) represents the nondissipative oscillation. The product of Eq. (62) and $(\Lambda^2 - 1)$ tends to $0+$ as $\Lambda^2 \rightarrow 1$, and thus the lhs of Eq. (40) is found to remain finite at $\Lambda^2 = 1$ with the aid of Eq. (46). Hence, we use Eq. (54) to find $d_1 = 1/K$ at $\Lambda^2 = 1$.

Below in this subsection, it is rather convenient to use

$$\Omega \equiv \frac{1}{\Lambda} = \frac{\omega \sqrt{\rho M}}{hk} \quad (63)$$

without using Λ . The second equality above comes from Eq. (47). We calculate d_1 numerically as stated below Eq. (62); d_1 depends on K and Ω^2 and can be referred to as $d_1(K, \Omega^2)$. In our numerical results, d_1 increases steeply as Ω^2 approaches the unity but the exact peak value cannot be obtained. This value is analytically found to be $1/K$ from the statement at the end of the preceding paragraph. The d_1 curve in each of Fig. 3(a) and (b) is drawn by connecting this exact peak value

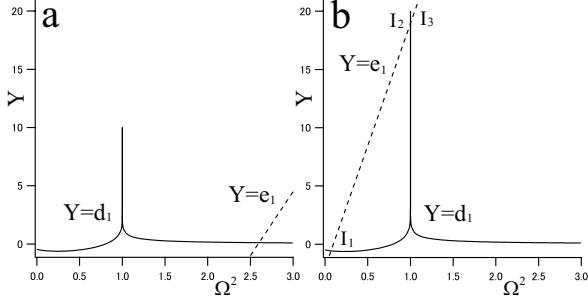


FIG. 3: The solid curves and dashed lines respectively represent $Y = d_1(K, \Omega^2)$ and $Y = e_1(K, \Omega^2)$ for $(\lambda, K) = (0.01, 0.1)$ (a) and $(0.025, 0.05)$ (b). These functions are defined by Eqs. (54) and (65). The slope of $Y = e_1$ is approximately given by $1/K$. Its Ω^2 intercept is given by the second entry of Eq. (66); its first term, $K^3/(4\lambda^2)$, equals 2.5 in (a) and 0.05 in (b). The minimum values of d_1 in (a) and (b) are -0.62 and -0.63 , respectively, at $\Omega^2 = 0.24$. In (b), we have $K^3 \ll K^2 = 4\lambda^2$, and the intersections are named as I_1 , I_2 , and I_3 .

and many other numerical outputs. The second term in the brackets on the rhs of Eq. (62) vanishes in the limit of $\Omega^2 \rightarrow 0+$. Thus, in this limit, $d_1(K, \Omega^2)$ becomes about $-1/2$ for small K , which can be read in Fig. 3. On the other hand, we assume small Λ^2 to derive Eq. (51), which means $d_1(K, \Omega^2) \rightarrow 0$ in the limit of $\Omega^2 \rightarrow \infty$. In Fig. 3, $d_1(K, \Omega^2)$ rapidly vanishes as Ω^2 increases beyond the unity. This can be understood from Eq. (62), as discussed below Eq. (B5).

Typically, we have $\rho_m^{(0)} \approx 10^{-7} \text{g/cm}^2$ [54], $\rho \approx 1 \text{g/cm}^3$, and $k^{-1} \gg 10^{-7} \text{cm}$, and thus can approximate $\rho_k^{(\text{eff})}$ as $2\rho/k$. Using this approximation, we divide Eq. (55) by $2c_b\lambda^2\tilde{\zeta}^{(1)}/\xi_c^4$ to obtain

$$K\Omega^2 = \frac{K^4}{4\lambda^2} + d_0(1 + d_1), \quad (64)$$

where we suppose $K \neq 0$ and $h \neq 0$. For a given value of K , the normal-mode frequency ω is determined by the solution of Eq. (64). It is given by the intersection of the curve $Y = d_1(K, \Omega^2)$ and

$$Y = \frac{K}{d_0(K)}\Omega^2 - \frac{K^4}{4\lambda^2 d_0(K)} - 1. \quad (65)$$

The rhs above is denoted by $e_1(K, \Omega^2)$, which also depends on λ^2 . The Y and Ω^2 intercepts of the line $Y = e_1$ are respectively given by

$$-\frac{K^2(K+1)}{4\lambda^2} - 1 \quad \text{and} \quad \frac{K^3}{4\lambda^2} + \frac{K}{K+1}, \quad (66)$$

which respectively tend to -1 and 0 as K decreases. We assume $K \equiv k\xi_c \ll 1$, as stated below Eq. (52).

In Fig. 3(a), there is one intersection and $\hat{\zeta}$ for a given vector \mathbf{k} is a normal mode. When the inequality $4\lambda^2 \ll K^3$ holds, the Ω^2 intercept of Eq. (66) is much larger than the unity and the intersection lies in the region where d_1 is almost constantly zero. This inequality is rewritten as $4h^2/(c_b M) \ll k^3$ with the aid of Eq. (47), and always holds when the membrane size is small enough to give $l_p^3 \ll 2\pi^3 c_b M/h^2$. Then, we can neglect d_1 in Eq. (55), and can derive Eqs. (52) and (53) from Eq. (51) in practice. We can predict the inequality condition from Eq. (51) without using Eqs. (40) and (57), as follows. Putting λ equal to zero and approximating $\rho_k^{(\text{eff})}$ as $2\rho/k$, we find the frequency determined by the bending energy to be $\sqrt{c_b k^5/\rho}/2$. We use this typical frequency as ω in Eq. (47) to find that the presupposed condition of $\Lambda^2 \ll 1$ gives $4\lambda^2 \ll K^3$. Judging from Fig. 3(a), if only when K^3 is larger than several times $4\lambda^2$, we can neglect d_1 . A larger membrane also contains modes satisfying $4\lambda^2 \lesssim K^3$. When this inequality is satisfied, the first term is much larger than the second term in the parentheses of Eq. (52) because of $4\lambda^2 \lesssim K^3 \ll K^2$. Thus, Eq. (53) is valid for modes of $4h^2/(c_b M) \lesssim k^3$ irrespective of the membrane size, but the suppression effect shown by the second term in its brackets is hard to observe owing to the predominant bending-energy term.

Let us consider a membrane large enough to contain modes satisfying $K^3 \ll 4\lambda^2$ and $K \ll 1$. For a mode of them, $Y = e_1$ and $Y = d_1$ have three intersections, as shown in Fig. 3(b), considering the intercepts in Eq. (66) and $e_1(K, 1) < 1/K$. They are referred to as I_1 , I_2 , and I_3 in the order of the proximity to the Y -axis although I_2 and I_3 cannot be distinguished in the figure. For a single value of k , these intersections give different values of the normal-mode frequency ω through Eq. (63). The mean square amplitude of a normal mode is smaller as the normal-mode frequency is larger in the equipartition theorem. Judging from the values of Ω^2 , the modes I_2 and I_3 have much larger ω than the mode I_1 in Fig. 3(b). There, regarding the modes I_2 and I_3 as immobile and noting $d_1 \approx -1/2$ for I_1 , from Eq. (55) we derive

$$\frac{2\rho}{k} \frac{\partial^2}{\partial t^2} \hat{\zeta}^{(1)} \approx - \left\{ \frac{c_b k^4}{2} + \frac{h^2}{M\xi_c} d_0(k\xi_c) \right\} \hat{\zeta}^{(1)}, \quad (67)$$

where $\rho_k^{(\text{eff})} \approx 2\rho/k$ is used. Here, the numerical factor of the term due to the ambient near-criticality is reduced to about half as compared with that of Eq. (52). Thus, we have Eq. (53) with the second term in the brackets being reduced to about half for modes satisfying $K^3 \ll 4\lambda^2$ and $K \equiv k\xi_c \ll 1$. The former inequality can be rewritten as $k^3 \ll 4h^2/(c_b M)$ with the aid of Eq. (47). In this result of the effective description, the suppression effect due to the ambient near-criticality can be observed because it overwhelms the one due to the bending rigidity when K is small enough to satisfy $K^2 \ll 2\lambda^2$, and thus can prevent a large tensionless

membrane from losing its orientation.

In Fig. 3(b), the Ω^2 intercept of Eq. (66) is much smaller than the unity because of $K^3 \ll 4\lambda^2$, and we can use the approximation $d_1(K, \Omega^2) \approx d_1(K, 0+) \approx -1/2$ at the intersection I_1 . Only when K decreases further to satisfy $K^2 \ll 2\lambda^2$, the term involving d_1 becomes relevant in Eq. (67). Then, all the more because K is smaller and the intersection approaches the Y -axis more, we can use the approximation better at the intersection. This discussion is much attributed to the k^4 -dependence of the bending energy. If we regard the mixture as a simple bath to calculate the mean square amplitude by using Eq. (1) naively, we obtain Eq. (53) with $d_0(K)$ being replaced by $1 - K_1^{-1}$, according to Eq. (A12) of Ref. 28. Here, K_1 is defined below Eq. (58). For $K \ll 1$, we have $1 - K_1^{-1} \approx K^2/2$, which also shows the reduction of the numerical factor to about half. This coincidence suggests that the ambient mixture can be regarded as a simple bath in the effective description for low energy (or small wavenumber) of a sufficiently large tensionless membrane. The transient profiles of the fields around a membrane undulating slowly in the reversible dynamics would be close to their respective equilibrium ones obtained when the membrane shape at each time is assumed to be fixed.

V. GENERAL FORMULATION FOR THE CRITICAL FRACTION

In this section, we assume that the mixture has the critical fraction far from the membrane and study the membrane undulation by taking into account cases where very near-critical mixture invalidates Eq. (44). Because φ_∞ equals the critical value of φ , the order parameter is defined as

$$\psi(\mathbf{r}) \equiv \varphi(\mathbf{r}) - \varphi_\infty, \quad (68)$$

which vanishes far from the membrane. We consider the mixture on the side of $z > 0$, as in Sec. IV. The reduced temperature, $\tau \equiv (T - T_c)/T_c$, is assumed to be positive. Below, $\beta \approx 0.326$, $\nu \approx 0.627$, $\gamma \approx 1.239$ and $\eta \approx 0.024$ are usual critical exponents for the three-dimensional Ising model, while ϵ denotes $4 - d$ in the ϵ -expansion; the dimension d is supposed to be three in this study. We write ξ_∞ for the correlation length far from the membrane. As stated above Eq. (45), it is given by $\xi_c \propto \tau^{-0.5}$ in the Gaussian model, which is not valid for sufficiently small τ . We have $\xi_\infty = \xi_0 \tau^{-\nu}$ in the leading behavior as $\tau \rightarrow 0+$, where ξ_0 is a nonuniversal constant. In the renormalized local functional theory [21], the correlation length ξ can be inhomogeneous and

$$w \equiv \xi_0^{1/\nu} \xi^{-1/\nu} \quad (69)$$

represents the local "distance" from the critical point.

In Eq. (1), considering that τ can be sufficiently small, $M(\varphi)$ should be given by

$$C(\psi) \equiv k_B T_c C_1 w^{-\eta\nu}, \quad (70)$$

where C_1 is a nonuniversal constant, while $f(\varphi)$ by [63]

$$f_R(\psi) \equiv k_B T_c \left\{ \frac{1}{2} C_1 \xi_0^{-2} w^{\gamma-1} \tau \psi^2 + \frac{1}{4} C_1^2 u^* \xi_0^{-\epsilon} w^{\gamma-2\beta} \psi^4 \right\}. \quad (71)$$

This is the same as Eq. (3.5) of Ref. 21 because of the scaling law $(\epsilon - 2\eta)\nu = \gamma - 2\beta$. The order parameter is not rescaled in the renormalized local functional theory, and thus f_s remains unchanged in the renormalization process. Because this free-energy functional is renormalized up to the local correlation length, we can use the mean-field theory to calculate ξ at each locus, which leads to

$$w = \tau + C_2 w^{1-2\beta} \psi^2, \quad (72)$$

where C_2 is a nonuniversal constant defined by

$$C_2 \equiv 3u^* C_1 \xi_0^{2-\epsilon}. \quad (73)$$

A rough estimate of u^* is $2\pi^2/9$ for $d = 3$. These equations can be found in Ref. 21; see its Eqs. (3.9) and (3.11) and the statement below its Eq. (3.16).

A. Interfacial properties in the unperturbed state

As discussed in Sec. IIB of Ref. 21, the profile minimizing Eq. (1) with Eqs. (70) and (71) is the equilibrium profile in the unperturbed state, for which we write ψ below unlike in the above. In other words, we below redefine ψ as

$$\psi(z) \equiv \varphi^{(0)}(z) - \varphi_\infty. \quad (74)$$

We can use Eqs. (14) and (15), which respectively become

$$C(\psi(z)) \left| \frac{d\psi(z)}{dz} \right|^2 = 2f_R(\psi(z)) \quad (75)$$

for $z > 0$, and

$$C(\psi(z)) \frac{d\psi(z)}{dz} = -h \quad (76)$$

as $z \rightarrow 0+$. Below in this section, we assume $h > 0$, which does not make us lose the generality. On this assumption, ψ decreases from a positive value to zero as z increases from zero to ∞ . Mathematically, ψ can diverge to ∞ at a negative z value, for which we write $-l$.

We can rewrite Eq. (72) as

$$U = 1 + s, \quad (77)$$

by defining

$$U \equiv w/\tau \quad \text{and} \quad s \equiv C_2 U^{1-2\beta} \tau^{-2\beta} \psi^2. \quad (78)$$

From the above, we immediately obtain

$$\frac{d\sqrt{s}}{dz} = \left(\frac{1}{2} - \beta\right) \frac{\sqrt{s}}{U} \frac{dU}{dz} + \frac{\sqrt{C_2}}{U^{\beta-(1/2)} \tau^\beta} \frac{d\psi}{dz}. \quad (79)$$

We find that it is convenient to rewrite Eq. (71) as

$$f_R(\psi) = \frac{k_B T_c C_1 \tau^{2\beta+\gamma}}{2C_2 \xi_0^2} U^{2\beta+\gamma-2} \left(s + \frac{s^2}{6}\right) \quad (80)$$

with the aid of Eqs. (73) and (78). We use Eqs. (70) and (75) to obtain

$$\frac{d\psi(z)}{dz} = -\frac{U^{\beta+\nu-1} \tau^{\beta+\nu}}{\sqrt{C_2} \xi_0} \left(s + \frac{s^2}{6}\right)^{1/2} \quad (81)$$

with the aid of the scaling law $\gamma + \eta\nu = 2\nu$.

We write $s(0+)$ for $s(z)$ in the limit of $z \rightarrow 0+$. Using Eqs. (70), (77), and (81), we can rewrite Eq. (76) as

$$\frac{\Theta}{\tau^{\beta+\nu-\eta\nu}} = \{1 + s(0+)\}^{\beta+\nu-\eta\nu-1} \left\{s(0+) + \frac{s(0+)^2}{6}\right\}^{1/2}, \quad (82)$$

where we use $\Theta \equiv \sqrt{C_2} \xi_0 h / (k_B T_c C_1)$. Substituting Eqs. (77) and (81) into Eq. (79), we obtain

$$-\xi_\infty \frac{d\sqrt{s}}{dz} = \frac{(1+s)^{\nu+(1/2)} \{s + (s^2/6)\}^{1/2}}{1+2\beta s}, \quad (83)$$

which implies that $s(z)$ decreases monotonically as z increases. Hence, we have

$$l = \xi_\infty \int_{s(0+)}^{\infty} ds \frac{1+2\beta s}{2(1+s)^{\nu+(1/2)} s \{1 + (s/6)\}^{1/2}}. \quad (84)$$

Let us suppose a mixture of nitroethane and 3-methylpentane, which has $T_c = 300$ K and $\xi_0 = 0.23$ nm [62]. In Ref. 19, the value of h is discussed on the assumption that one component of the mixture interacts with a wall made of glass through the hydrogen bonding, which leads to $h \approx 10^{-6}$ m³/s² [28]. This estimate would be overestimated for a membrane, which cannot make hydrogen bonding so much. The coefficient of the square gradient term in the free-energy density is sometimes called influence parameter [57, 58]. The parameter can be defined in general for each pair of the components, A - A , B - B , and A - B , where A and B represent the kinds of the two components. The coefficient M is for the last pair, which can be roughly given by the geometric mean of the parameters for the first two pairs [59]. In Eq. (70),

$$w^{-\eta\nu} \approx w^{-0.015} \quad (85)$$

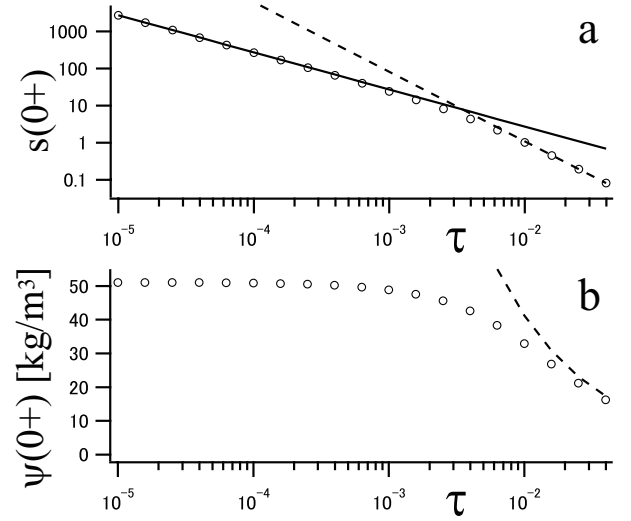


FIG. 4: We use $h = 10^{-6}$ m³/s² and other parameter values described in the text. (a) Numerical results of $s(0+)$, obtained from Eq. (82), are plotted against τ with circles. The solid line represents Eq. (88), while the dashed line represents Eq. (87). (b) Numerical results of $\psi(0+)$ are plotted against τ (circles). See Eq. (74) for the definition of ψ . The values are smaller than the mass density of the mixture $\approx 10^3$ kg/m³, as ψ should be. The dashed curve is calculated from Eq. (45), where M and ξ_c are respectively regarded as $k_B T C_1$ and $\xi_0 \tau^{-\nu}$.

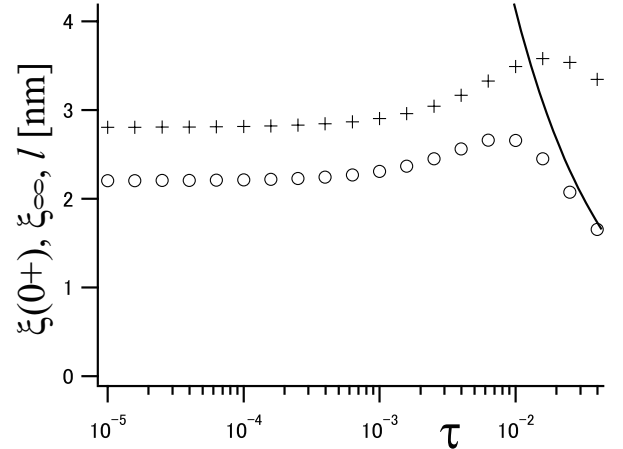


FIG. 5: Crosses and circles represent numerical results of l and $\xi(0+)$, respectively. They are obtained from Eqs. (84) and (86). The solid curve represents $\xi_\infty = \xi_0 \tau^{-\nu}$, which reaches 2×10 nm at $\tau = 10^{-3}$ and 7×10 nm at $\tau = 10^{-4}$. The parameter values are the same as used in Fig. 4.

can be regarded as approximately the unity for the temperature range considered in the following graphs. We cannot find out the data of the influence parameters for the mixture mentioned above, but can estimate $k_B T C_1 = 10^{-16}$ m⁷/s²kg for this mixture or a similar mixture from the data for the pure fluid of alkane [60, 61].

Using these estimates, we solve Eq. (82) numerically and plot the results with circles in Fig. 4(a). Substituting these numerical results into the second equation of Eq. (78) with the aid of Eq. (77), we obtain the results represented by the circles of Fig. 4(b). Using the results of $s(0+)$, we calculate Eq. (84) numerically to plot the results with crosses in Fig. 5,. Using Eq. (77) and the first equation of Eq. (78), we have $w = \tau(1 + s)$. Combining this with Eq. (69), we find that the value of ξ at $z \rightarrow 0+$, denoted by $\xi(0+)$, is given by

$$\xi(0+) = \xi_0 \{\tau(1 + s(0+))\}^{-\nu}, \quad (86)$$

which is plotted in Fig. 5. For reference, there we also plot ξ_∞ , the correlation length far from the membrane.

When $s(0+)$ is much smaller than the unity, Eq. (82) gives

$$s(0+) \approx \Theta^2 \tau^{-2(\beta+\nu-\nu\eta)}, \quad (87)$$

which is plotted with the dashed line in Fig. 4(a). The approximation turns out to work well in the region of $\tau > 10^{-2}$, where $s(0+)$ is smaller than the unity. There, ξ_∞ is approximately equal to $\xi(0+)$ in Fig. 5. As τ decreases further, $\xi(0+)$ becomes much shorter than ξ_∞ . As τ decreases down to about 10^{-3} in Fig. 4(b), $\psi(0+)$ increases and deviates more from the critical value, *i.e.*, zero. Because of the surface field, the mixture near the membrane is not so close to the critical point as the mixture far from the membrane. As τ decreases further, $\psi(0+)$ becomes independent of τ , and then l and $\xi(0+)$ also become independent in Fig. 5. The existence of this plateau of $\psi(0+)$ cannot be expected from Eq. (45) in the Gaussian model, where $\psi(0+) = h\xi_c/M$ increases with the correlation length. See the dashed curve in Fig. 4(b) for this increase. We use a smaller value of h to plot the same quantities in Figs. 6 and 7. The region where Eq. (87) works well extends to smaller τ , the plateau value of $\psi(0+)$ is smaller, the plateau values of l and $\xi(0+)$ are larger, and the plateau regions appear only for smaller τ values. These behaviors of $\psi(0+)$ and $\xi(0+)$ imply that the mixture near the membrane is closer to the critical point and is more similar to the mixture far from the membrane when h is smaller for sufficiently small τ .

Let us assume $\tau(> 0)$ to be small enough to give $s(0+) \gg 1$. Then, the rhs of Eq. (82) is approximated to be $s^{\beta+\nu-\nu\eta}/\sqrt{6}$, which leads to

$$s(0+) \approx (\sqrt{6}\Theta)^{1/(\beta+\nu-\nu\eta)} \tau^{-1}, \quad (88)$$

which is drawn with the solid line in Figs. 4(a) and 6(a). The approximation turns out to work well when $s(0+)$ is much larger than the unity. Using Eq. (77) and the second equation of Eq. (78), we have

$$(\sigma\tau)^\beta \approx \sqrt{C_2}\psi \quad (89)$$

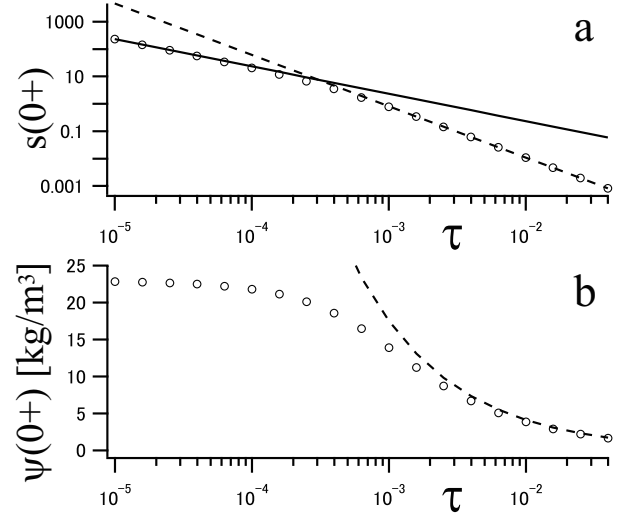


FIG. 6: This figure is drawn in the same way as Fig. 4, except for $h = 10^{-7} \text{ m}^3/\text{s}^2$.

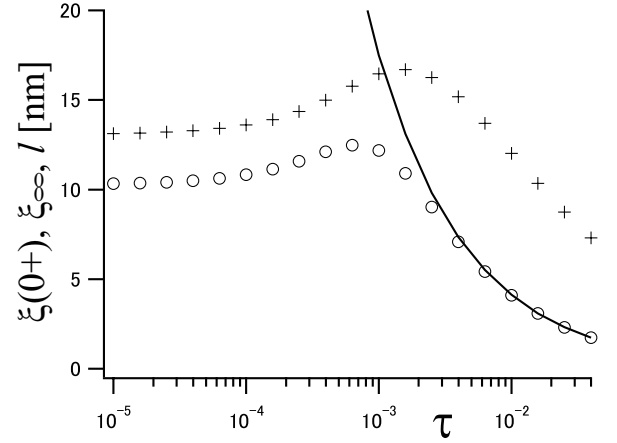


FIG. 7: This figure is drawn in the same way as Fig. 5, except for $h = 10^{-7} \text{ m}^3/\text{s}^2$. The solid curve remains the same because ξ_∞ is independent of h .

for $s \gg 1$. Thus, when $s(0+)$ is much larger than the unity, we use Eq. (88) to obtain

$$\psi(0+) \approx \frac{1}{\sqrt{C_2}} (\sqrt{6}\Theta)^{\beta/(\beta+\nu-\nu\eta)}, \quad (90)$$

which equals $5.1 \times 10 \text{ kg/m}^3$ and $2.3 \times 10 \text{ kg/m}^3$ for the material constants used in Figs. 4(b) and 6(b), respectively. These values agree with the plateau values in the respective figures. When $s(0+)$ is sufficiently large, the rhs of Eq. (84) reads

$$\sqrt{6}\beta\xi_\infty \int_{s(0+)}^{\infty} ds \frac{1}{s^{\nu+1}}. \quad (91)$$

Substituting Eq. (88) into Eq. (91), we find Eq. (84) to

give

$$l \approx \frac{\sqrt{6}\beta\xi_0}{\nu} \left(\frac{1}{\sqrt{6}\Theta} \right)^{\nu/(\beta+\nu-\nu\eta)}, \quad (92)$$

which equals 2.8 nm and 1.3×10 nm for the material constants used in Figs. 5(b) and 7(b), respectively. These values agree with the plateau values in the respective figures. Because of Eqs. (86), (88), and (92), the plateau values of l and $\xi(0+)$ turns out to be related by

$$l \approx \frac{\sqrt{6}\beta\xi(0+)}{\nu}, \quad (93)$$

which is approximately equal to $1.27\xi(0+)$. This can be read in Figs. 5(b) and 7(b).

B. Order-parameter profile in the unperturbed state

Because $s(z)$ decreases monotonically down to zero as z increases, we have $s(z) \ll 1$ beyond a value of z however small $\tau(>0)$ may be. There, noting $U \approx 1$, we substitute the second equation of Eq. (78) into Eq. (81) and obtain

$$\frac{d\psi}{dz} \approx -\frac{\psi}{\xi_\infty}, \text{ i.e., } \psi(z) \propto e^{-z/\xi_\infty}. \quad (94)$$

Hence, the same exponential decay as that of Eq. (45) in the Gaussian model appears beyond some distance from the membrane even if τ is sufficiently small, which is well known [34, 37]. When τ is large enough to give $s(0+) \ll 1$, Eq. (94) naturally appears from immediately near the membrane. This can be explained alternatively as follows. Considering Eqs. (77) and (78), we find that the rhs of Eq. (80) becomes $C(\psi)\psi^2/(2\xi_\infty^2)$ approximately if $s(0+)$, and thus $s(z)$, are much smaller than the unity. Thus, regarding C and ξ_∞ as M and ξ_c , respectively, and noting the remark of Ref. 63, we find that the Gaussian model Eq. (44) is available when $s(0+) \ll 1$ holds. Then, we use Eqs. (14) and (15) to obtain Eq. (45). The spacial region where Eq. (94) appears is detached from the membrane when τ is small enough to give $s(0+) \gg 1$. Then, the difference in the distance from the critical point between the mixture near the membrane and the one far from the membrane becomes significant. For this reason, ξ_∞ deviates from $\xi(0+)$ for small values of τ in Figs. 5 and 7.

An alternative way to Eq. (92) is from Eq. (81), as shown below. Let us assume $s(0+)$ to be much larger than the unity. We have $s(z) \gg 1$ up to a positive value of z . There, because of $U \approx s$, Eq. (81) leads to

$$\frac{d\psi(z)}{dz} \approx \frac{(s\tau)^{\beta+\nu}}{\sqrt{6}C_2\xi_0}. \quad (95)$$

Thus, using Eq. (89), we find

$$\psi(z) \approx \frac{1}{\sqrt{C_2}} \left\{ \frac{\sqrt{6}\beta\xi_0}{\nu(z+l_0)} \right\}^{\beta/\nu} \quad (96)$$

with l_0 being a constant. Noting that $d\psi/(dz)$ equals $-\beta\psi(0+)/(\nu l_0)$ at $z = 0+$, we use Eqs. (70), (76), and (89) to find l_0 to be given by Eq. (92), i.e., $l_0 = l$. The profile of Eq. (96) is the same as Eq. (2.15) of Ref. 21 for $\tau = 0$ and $\psi(\infty) = 0$ because of the statement below its Eq. (3.15).

Suppose that τ is small enough to give $l \ll \xi_\infty$. Judging from Eqs. (89) and (96), $s(z)$ is reduced to the unity at $z \approx \xi_\infty$, i.e., $s(z)$ is much larger than the unity for $z \ll \xi_\infty$. Thus, in the range of $l \ll z \ll \xi_\infty$, from Eq. (96) we have approximately

$$\psi(z) \propto \left(\frac{\xi_0}{z} \right)^{\beta/\nu} = \tau^\beta \left(\frac{z}{\xi_\infty} \right)^{-\beta/\nu}, \quad (97)$$

which is consistent with the universal form [33, 34, 37, 40]. The origin appears to be shifted by the distance l , which is negligible for the range of z considered here. This shift, as well as the range of z , is pointed out in Refs. 36 and 37. For sufficiently small τ , the range of z where Eq. (97) holds emerges. Neglecting l amounts to assuming $\psi(0+)$ and h to diverge, considering Eqs. (90) and (92). It is thus reasonable that they appear to diverge in some ways of deriving Eq. (97). However, in the way shown above, we do not assume them to diverge in deriving Eq. (96), which leads to Eq. (97).

Solving Eqs. (82) and (83) numerically, we use Eq. (78) to calculate $\psi(z)$. In Fig. 8, where τ is sufficiently small, we find Eq. (96) to give a good approximation for small z . As z is larger in this figure, the numerical results agree with Eq. (94) although Eq. (45) with M and ξ_c being respectively replaced by $k_B T C_1$ and $\xi_0 \tau^{-\nu}$ is much larger than the numerical results (though data not shown). In the renormalized local functional theory, the local coarse-graining is performed up to ξ , and thus up to $\xi(0+)$ near the membrane. When the mixture is very close to the critical point, the values of l and $\xi(0+)$ are comparable in Eq. (93), and thus the nonzero value of l cannot be neglected altogether. The numerical results for other values of τ are plotted in Fig. 9. In its (a), neither Eq. (45) nor Eq. (96) gives a good approximation; in its (b), τ is sufficiently large and Eq. (45) gives a good approximation. For these large values of τ , Eq. (96) cannot explain the numerical results for $z > 0$ and l becomes meaningless.

In the renormalized local functional theory, the well-known universal property does not contradict with a finite surface field [64]. The gradient of the order parameter remains moderate, even near the membrane,

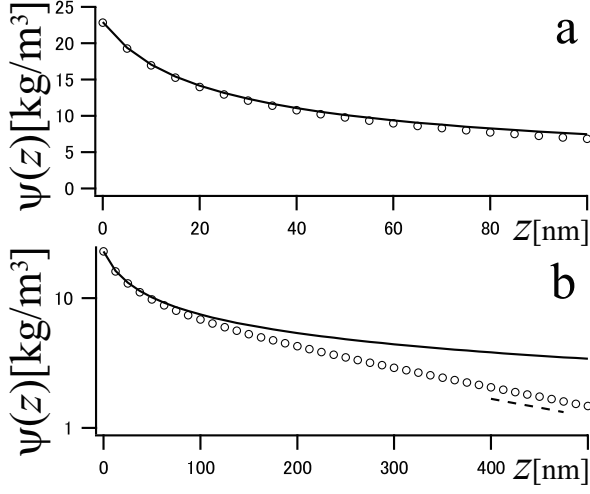


FIG. 8: Circles represent the numerical results of $\psi(z)$, which is defined by Eq. (74). The solid curve represents Eq. (96). We use $\tau = 10^{-5}$, $h = 10^{-7} \text{ m}^3/\text{s}^2$ and the other material constants stated in the text, which give $\xi_\infty = 3.14 \times 10^2 \text{ nm}$. The linear plot is given in (a), while the logarithmic plot for a wider range is given in (b), where the dashed line represents the slope of $-1/\xi_\infty$.

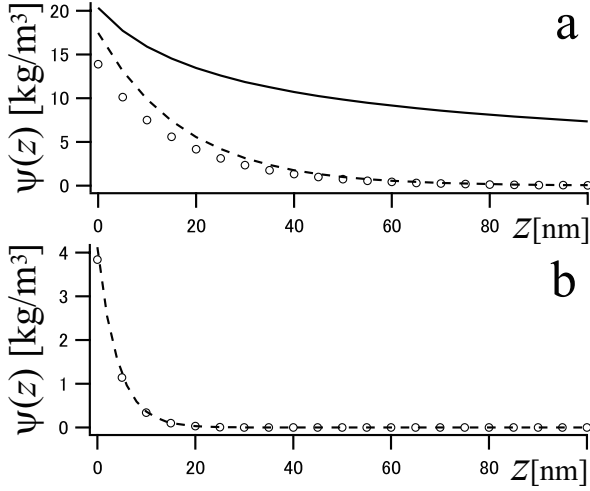


FIG. 9: Circles represent the numerical results of $\psi(z)$, the solid curve represents Eq. (96), and the dashed curve represents Eq. (45) with M and ξ_c being respectively replaced by $k_B T C_1$ and $\xi_0 \tau^{-\nu}$. The same parameter values are used as in Fig. 8, except for $\tau = 10^{-3}$ in (a) and 10^{-2} in (b). These values respectively give $\xi_\infty = 1.75 \times 10 \text{ nm}$ and $\xi_\infty = 4.13 \text{ nm}$.

as the temperature approaches T_c . Thus, we can formulate the hydrodynamics for a near-critical binary fluid mixture in terms of the renormalized local functional theory with a finite surface field.

C. Application to the undulation amplitude

Hereafter, we assume $\xi_a = \xi(0+)$ to have $K = k\xi(0+)$. This does not contradict with $\xi_a = \xi_c$ assumed in Sec. IV because $\xi(0+)$ can be identified with ξ_∞ when the Gaussian model is valid, as shown in Figs. 5 and 7, and because ξ_∞ is given by ξ_c in the Gaussian model. It is convenient to use $\xi(0+)$ as a length unit because it reaches a plateau as τ becomes sufficiently small, unlike ξ_∞ . From Eqs. (28) and (33), we obtain

$$\left(1 - \frac{M_{00}}{M_0 \Lambda^2 \Xi^2}\right) (\partial_Z^2 - K^2) U_{\text{out}} = - \left\{ \frac{M'_0 \psi' \xi(0+)}{M_0} + \frac{2\Xi'}{\Xi} \right\} \partial_Z U_{\text{out}}, \quad (98)$$

which is reduced to Eq. (57) in the Gaussian model. Here, M_{00} denotes $C(\psi(0+))$; $M_0 \equiv C(\psi(z))$ and Ξ are determined by $\psi(z)$, which is the solution of Eqs. (82) and (83). The boundary conditions remain the same as stated below Eq. (57), and are given at $Z \rightarrow 0+$ and $Z \rightarrow \infty$. Because of Eq. (75), $M_0 \Xi^2$ is proportional to $f_R(\psi(z))$ and decrease to zero as z increases to ∞ . Thus, when $\Lambda^2 \Xi(0+)^2$ is larger than the unity, the difference in the first parentheses on the lhs of Eq. (98) vanishes at a value of Z making $M_0 \Lambda^2 \Xi^2$ equal to M_{00} , and U_{out} would have some singularity there, considering the results of Sec. IV B. Hence, when Λ^2 is sufficiently large, it should be difficult to obtain the full solution of Eq. (98) not only analytically but also numerically.

In the Gaussian model discussed in Sec. IV B, the suppression effect due to the bending rigidity overwhelms the one due to the ambient near-criticality derived on the assumption of a weak surface field. To examine whether this situation continues and how the restoring force depends on the correlation length beyond the regime of the Gaussian model, we below assume sufficiently small $|\Lambda|$ to study the undulation amplitude by using the renormalized local functional theory. As in Sec. IV A, we use Eq. (31) in Eq. (33) to obtain Q_{out} up to the order of Λ . Substituting this result into Eq. (34), we use the integration by parts and Eq. (70) to obtain

$$\lim_{Z \rightarrow 0+} \partial_Z U_{\text{out}} = -K - \Lambda^2 \Xi(0+)^2 K + \frac{k^2 \xi(0+)}{\rho \omega^2} D(k) \quad (99)$$

up to the order of Λ^3 , like Eq. (48). Here, we use

$$D(k) \equiv 2k^2 \int_0^\infty dz e^{-2kz} C(\psi(z)) \psi'(z)^2 \quad (100)$$

$$= 4k^2 \int_0^\infty dz e^{-2kz} f_R(\psi(z)), \quad (101)$$

the second equality of which comes from Eq. (75). Using Eqs. (40), (41), (42), and (99), for a tensionless membrane, we obtain

$$\rho_k^{(\text{eff})} \omega^2 \tilde{\zeta}^{(1)} = \left\{ \frac{c_b k^4}{2} + 2D(k) \right\} \tilde{\zeta}^{(1)}, \quad (102)$$

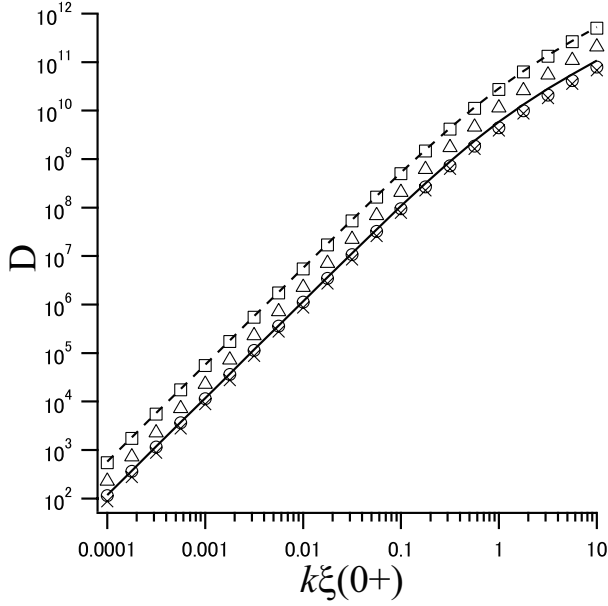


FIG. 10: For $\tau = 10^{-5}$ (\circ), 10^{-3} (\times), 10^{-2} (\triangle), $10^{-1.4}$ (\square), we plot the numerical results of Eq. (101) against $k\xi(0+)$. The solid curve represents $\bar{D}(k\xi(0+))$ for $\tau = 10^{-5}$. The dashed curve represents the lhs of Eq. (103) with M and ξ_c being respectively replaced by $k_B T C_1$ and $\xi_0 \tau^{-\nu}$. We use $h = 10^{-7} \text{ m}^3/\text{s}^2$ and the other material constants stated in Sec. V A.

where higher-order terms with respect to Λ are neglected. As discussed in Appendix C, Λ is still almost proportional to h for sufficiently small τ . If σ_1 does not vanish, $\sigma_1 k^2$ is added to the sum in the brackets of Eq. (102). When we assume the Gaussian model to use Eq. (45) in Eq. (100), Eq. (102) is reduced to Eq. (51), and then $D(k)$ becomes

$$\frac{h^2 d_0(k\xi_c)}{M\xi_c} \approx \frac{h^2 k^2 \xi_c}{M}. \quad (103)$$

We can use Eqs. (77) and (80) in Eq. (101), the numerical integration of which requires $s(z)$. We obtain $s(z)$ by solving Eqs. (82) and (83) numerically for smaller values of z and by utilizing Eq. (94) for larger values of z . Using the results, we plot $D(k)$ against $k\xi(0+)$ for some values of τ in Fig. 10. The results for $\tau = 10^{-1.4}$ agree with the dashed curve representing the corresponding result in the Gaussian model, *i.e.*, representing the lhs of Eq. (103) plotted against $k\xi_c = k\xi_\infty$, which can be regarded as $k\xi(0+)$ at this temperature as is shown in Fig. 7.

Let us assume that τ is small enough to give $s(z) \gg 1$ up to a sufficiently large value of z . Then, the contribution from the region beyond this z value is negligible in the integral of Eq. (101). Thus, assuming $s \gg 1$, we use Eq. (80) in the integrand to obtain Eq. (C1), which leads

to

$$D(k) \approx \frac{\sqrt{6}\beta}{4\nu\pi^2} \times \frac{k_B T_c k^2}{\xi(0+)^2} \quad (104)$$

when $kl \ll 1$. If h vanishes, Eq. (104) becomes meaningless because even $s(0+)$ cannot be much larger than the unity however small τ may be. Equations (100), (101), and (104) can be derived as they are even if ξ_a is not specified as $\xi(0+)$. This is reasonable because Eq. (102) should be independent of the way of nondimensionalization. We define $\bar{D}(k)$ as the rhs of Eq. (104) with k^2 being replaced by $d_0(k\xi(0+))/\xi(0+)^2$. When $k\xi(0+) \ll 1$ holds, $\bar{D}(k)$ can be identified with the rhs of Eq. (104). Then, $\bar{D}(k)$ agrees well with the numerical results of Eq. (101) for $\tau = 10^{-5}$ in Fig. 10, as is expected. The figure also shows that the agreement remains fairly good when $k\xi(0+)$ is larger, which means that the dependence of Eq. (101) on k can be almost described by $d_0(k\xi(0+))$ even when τ is sufficiently small.

We find in Fig. 10 that Eq. (101) remains almost unchanged when τ changes from 10^{-5} to 10^{-3} . This is also shown by circles in Fig. 11, where Eq. (101) for $k\xi(0+) = 10^{-2}$ almost reaches a plateau in this region of τ and the plateau value agrees with Eq. (104). In this region of τ , $\xi(0+)$ almost reaches a plateau in Fig. 7. For values of τ larger than about 10^{-3} in Fig. 11, the circles agree well with the dashed line, which represents the lhs of Eq. (103) with $k\xi_c = 10^{-2}$. For these values of τ , ξ_∞ coincides with $\xi(0+)$ in Fig. 7. It is thus expected that we can obtain $D(k)$ over a wide range of τ by regarding ξ_c as $\xi(0+)$ in the result of the Gaussian model, the lhs of Eq. (103). This expectation is roughly correct, as discussed in the next paragraph. Not ξ_∞ but $\xi(0+)$ is relevant in Eq. (102), which is reasonable considering that the hydrodynamics near the membrane is important to the stress exerted on the membrane and that the mixture far from the membrane can be regarded as a bath. Thus, in general $k\xi(0+) \ll 1$ should be required for the validity of our hydrodynamic formulation; this condition becomes $k\xi_c \ll 1$ mentioned below Eq. (52) in the Gaussian model.

We use Eqs. (86) and (88) to obtain

$$\xi(0+) \approx \xi_0 \left(\frac{k_B T_c \sqrt{C_1}}{2\pi h \xi_0^{3/2}} \right)^{\nu/(\beta+\nu-\nu\eta)} \quad (105)$$

when τ is sufficiently small. The power in the above is approximately $2/3$ because the scaling law and the hyperscaling law give $2\beta/\nu = 1 + \eta$. Using this approximate power, we can rewrite Eq. (104) as

$$D(k) \approx \frac{h^2 k^2 l}{k_B T_c C_1} \quad (106)$$

with the aid of Eq. (93). As mentioned around Eq. (85), $k_B T_c C_1$ is regarded as M . Considering that l is roughly

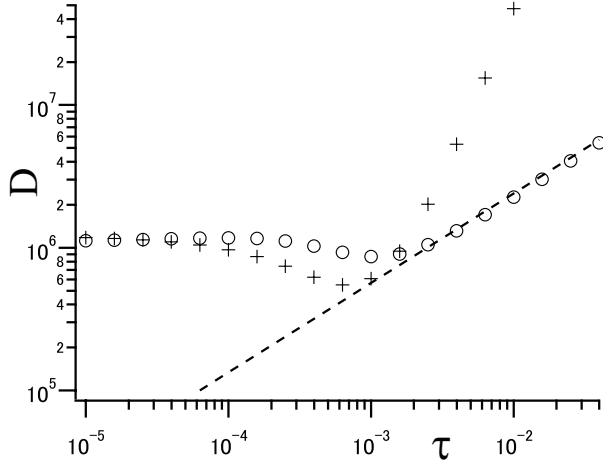


FIG. 11: Circles represent the numerical results of Eq. (101) for $k\xi(0+) = 10^{-2}$, and crosses represent Eq. (104) for $k\xi(0+) = 10^{-2}$. The dashed line represents the corresponding result in the Gaussian model, $h^2 d_0(10^{-2})/(k_B T_c C_1)$. We use the same material constants as in Fig. 10.

equal to $\xi(0+)$ in Eq. (93), we can obtain Eq. (106), *i.e.*, Eq. (104), roughly by regarding ξ_c by $\xi(0+)$ in the lhs of Eq. (103) when $k\xi(0+)$ is small. See Appendix C for an alternative discussion. Considering the fairly good agreement between \bar{D} and the numerical results for small τ in Fig. 10, whether $k\xi(0+)$ is small or not, we can obtain Eq. (101) roughly by regarding ξ_c as $\xi(0+)$ in the lhs of Eq. (103).

As discussed in the sixth paragraph of Sec. IV B, we can use the typical frequency of the bending energy to arrive at the condition for Eq. (52) without using the solution of Eq. (57). Applying this discussion on the typical frequency to Eq. (27) with ξ_a being replaced by $\xi(0+)$, we arrive at $4\lambda^2 \ll \{k\xi(0+)\}^3$. This inequality condition is consistent with the value of Z making Eq. (98) singular, as discussed at the end of Appendix C. Thus, for modes satisfying $4\lambda^2 \ll \{k\xi(0+)\}^3$ in a tensionless membrane, we can rewrite Eq. (102) as

$$\frac{2\rho}{k} \frac{\partial^2}{\partial t^2} \hat{\zeta}^{(1)} \approx - \left\{ \frac{c_b k^4}{2} + 2D(k) \right\} \hat{\zeta}^{(1)}, \quad (107)$$

where $\rho_k^{(\text{eff})} \approx 2\rho/k$ is used. For a wavenumber satisfying the inequality, the mean square amplitude is thus given by Eq. (53) with the second term in the brackets being replaced by $2D(k)$, and the ambient near-criticality tends to suppress the undulation amplitude because Eq. (100) is positive. However, considering the approximate expression of $D(k)$ mentioned in the preceding paragraph, whenever the inequality condition is satisfied, the first term is much larger than the second term in the brackets of Eq. (107). Thus, as in the Gaussian model, the suppression effect for $4\lambda^2 \ll \{k\xi(0+)\}^3$ is hard to observe because of the predominant bending-energy

term.

In the Gaussian model discussed in Sec. IV B, we can solve Eq. (57) to discuss the undulation amplitude for large Λ^2 . The corresponding equation here, Eq. (98), is not solved. However, an approximate discussion on Eq. (98) for small K , given in Appendix D, shows that $d_1(K, \Omega^2)$ in the limit of $\Omega^2 \rightarrow 0+$ remains equal to about $-1/2$. It is thus suggested, as in the Gaussian model, that the numerical factor of D of Eq. (107) should be reduced from two to about the unity in the effective low-energy description which is valid for modes satisfying $\{k\xi(0+)\}^3 \ll 4\lambda^2$ and $k\xi(0+) \ll 1$ in a large tensionless membrane. The reduction to about half should be supported by the naive average calculated from the renormalized free-energy functional on the assumption that the mixture is a simple bath, judging from the discussion in the last paragraph of Sec. IV B. In Appendix E, we calculate the mean square amplitude on this assumption in an approximate way for small wavenumber. The result also shows the reduction to about half. It is thus strongly suggested that Eq. (53) with the second term in the brackets being replaced by $D(k)$ of Eq. (100) is valid for modes satisfying $\{k\xi(0+)\}^3 \ll 4\lambda^2$ and $k\xi(0+) \ll 1$ in a large tensionless membrane not only in the Gaussian model but also beyond its regime. In this result, the suppression effect due to the ambient-near criticality can overwhelm that of the bending energy and be observed; it can prevent a large tensionless membrane from losing its orientation over a wide temperature range. For sufficiently small τ , we use Eq. (C5) to rewrite $\{k\xi(0+)\}^3 \ll 4\lambda^2$ as $k^3 \ll 5.6h^2/(c_b M)$, which is not much different from the corresponding inequality in the Gaussian model pointed out below Eq. (67).

VI. SUMMARY AND OUTLOOK

We consider how the mean square amplitude of the shape fluctuation of a fluid membrane is modified by the ambient near-criticality. This is an equal-time correlation, and the mixture far from the membrane can be regarded as a heat and particle bath. However, the mixture near the membrane is closely linked with the membrane and cannot be regarded as a part of the bath. We can find out the contribution from this part to the shape fluctuation by utilizing the reversible hydrodynamics; this amounts to detecting what part moves by shaking the membrane. In Fig. 2, the transient density profile in the mixture does not always agree with the equilibrium one calculated on the assumption that the wavy membrane is fixed as it is. Even on this assumption, the deformed profile generates the restoring force, but it cannot be expected to give the genuine one for the fluctuating membrane. The calculation becomes complicated partly because of the boundary-layer prob-

lem in the limit of the vanishing interdiffusion.

Previously, the present author calculated the mean square amplitude by assuming the Gaussian model with weak preferential attraction [28]. According to the result for a tensionless membrane, Eq. (52), the restoring force due to the ambient near-criticality tends to suppress the undulation, increases with the correlation length far from the membrane ξ_c , and has the k^2 -dependence for $k\xi_c \ll 1$, where the coarse-grained formulation is valid. The calculation in this previous study contains solving Eq. (16) for the Gaussian model. In the present study, we look at only its interfacial property to derive Eq. (36), which holds even if the Gaussian model is not assumed. This interfacial property leads to Eq. (40), which links the outer solution to the stress exerted on the membrane. On the other hand, because of the interfacial property, it becomes unnecessary to solve Eq. (16), which opens a way of studying beyond the Gaussian model.

In Sec. IVB, we derive Eq. (57), a closed equation for the outer solution of $\tilde{V}_z^{(1)}$, in the Gaussian model without imposing any assumption on the strength of the surface field. We use its solution to draw Fig. 3, where an intersection of the curve and line gives a normal-mode frequency. First, the previous result, Eq. (52), turns out to be valid only when $4\lambda^2 \lesssim (k\xi_c)^3$, *i.e.*, $4h^2/(c_b M) \lesssim k^3$, holds. The resultant suppression effect due to the ambient near-criticality, represented by the second term in the brackets of Eq. (53), is hard to observe because of the predominant bending-energy term. Second, for a mode of $k^3 \ll 4h^2/(c_b M)$ in a large tensionless membrane, we find that the restoring force in Eq. (52) effectively remains although the numerical factor is reduced to about half. This suppression effect for small wavenumber can overwhelm the one due to the bending-energy term and can be observed in practice. It can prevent a large tensionless membrane from losing its orientation. It is also elucidated that we can regard the mixture as a simple bath in this effective description for low energy.

In Sec. V, assuming that the mixture far from the membrane has the critical fraction in the homogeneous phase, we consider the undulation by utilizing the renormalized local functional theory valid in a wider temperature range than considered in the Gaussian model. We write ξ_∞ for the correlation length far from the membrane in general because ξ_c is defined only in the Gaussian model. Equation (80) enables us to make the calculation procedure concise. The unperturbed state is discussed in the first two subsections, where it is shown that we can derive the well-known universality by assuming a finite surface field. When the Gaussian model ceases to be valid is discussed by means of Figs. 4 and 6. As τ decreases beyond the regime of

the Gaussian model, the correlation length near the membrane, $\xi(0+)$, deviates from ξ_∞ , and finally reaches a plateau value, which is about 2 nm in Fig. 5 and about 10 nm in Fig. 7. This is because the mixture near the membrane remains away from the critical point because of the preferential attraction. In Sec. VC, we calculate the mean square amplitude in the framework of the renormalized local functional theory with sufficiently weak surface field, noting that a finite surface field is shown to be available in the preceding subsections. It is revealed that the result of Eq. (107) is roughly the same as the corresponding result in the Gaussian model, Eq. (52), if the correlation length ξ_c is interpreted as $\xi(0+)$. The resultant suppression effect due to the ambient near-criticality in this framework is suggested to be valid only for large wavenumber and hard to observe because of the predominant bending-energy term, as in the Gaussian model.

In the last paragraph of Sec. VC, we discuss the undulation with small wavenumber in the framework of the renormalized local functional theory. It is also suggested that, although the numerical factor is reduced to about half, the restoring force derived for large-wavenumber modes mentioned in the preceding paragraph effectively remains for $\{k\xi(0+)\}^3 \ll 4\lambda^2$ and $k\xi(0+) \ll 1$. The resultant suppression effect can be observed; the situation is the same as in the Gaussian model but the restoring force involves $\xi(0+)$. When the temperature approaches the critical one, $\xi(0+)$ reaches a plateau and the undulation amplitude is not totally suppressed by the ambient near-criticality. This is against the anticipation we have in the Gaussian model.

For the membrane with the inverted polarity, mentioned in the first paragraph of Sec. I, the bending rigidity c_b is reported to be around 2×10^{-20} J [65]. Using $h = 10^{-7}$ m³/s² and $M = 10^{-16}$ m⁷/(s²kg) mentioned in Sec. VA, we have $4h^2/(c_b M) = 2 \times 10^{22}$ m⁻³ and can expect that the effective description for low energy is valid for a membrane having the size much larger than about 200 nm within and beyond the regime of the Gaussian model. The size considered here is so small that c_b can be regarded as independent of the membrane size [8–10]. The suppression effect due to the ambient near-criticality overwhelms the one due to the bending energy and can be observed when k is smaller than $2h^2\xi(0+)/(c_b M)$, which equals 5 and 10 μm^{-1} for $\xi(0+) = 3$ and 10 nm, respectively.

Our results beyond the regime of the Gaussian model supposes the critical fraction far from the membrane. When the fraction is otherwise tuned appropriately, sufficiently large $\xi(0+)$ may suppress the undulation totally or may make the undulation unstable with the aid of substantial preferential attraction. As the mixture becomes extremely close to the critical point, its concentration fluctuation may be significant to the

undulation modes of $k\xi(0+) \gg 1$ in spite of the strong suppression due to the bending energy. This can affect the mean square amplitude at a point, $\langle \zeta(\mathbf{x}, t)^2 \rangle$. These problems wait future studies.

Acknowledgments

The author thanks Professor Shun Shimomura for helpful information on the analytical continuation of the hypergeometric function.

Appendix A: Some details in Sec. III.

In Eq. (16), N is defined as

$$N(z) \equiv -f''(\varphi^{(0)}) + M_0' \varphi^{(0)''} + \frac{1}{2} M_0'' \left| \varphi^{(0)'} \right|^2. \quad (\text{A1})$$

Multiplying the x - and y -components of the Fourier transforms of Eq. (6) with k_x and k_y , respectively, and substituting the Fourier transform of Eq. (5) into their sum, we obtain

$$\frac{\rho\omega}{k} \frac{\partial}{\partial z} \tilde{V}_z^{(1)} = -ik\tilde{p}^{(1)} - ik\varphi^{(0)} \tilde{\mu}^{(1)}. \quad (\text{A2})$$

From the z -component of Eq. (6) and the derivative of Eq. (A2) with respect to z , we delete $\partial\tilde{p}^{(1)}/\partial z$ to obtain

$$\left(\frac{\partial^2}{\partial z^2} - k^2 \right) \tilde{V}_z^{(1)} = -\frac{ik^2}{\rho\omega} \varphi^{(0)'} \tilde{\mu}^{(1)} \quad (\text{A3})$$

for $z \neq 0$. The same procedure is taken when Eq. (41) is derived in Ref. 28.

Substituting Eq. (13) into Eq. (8), we pick up terms at the order of ε to obtain

$$\frac{\partial \varphi^{(1)}}{\partial t} = -V_z^{(1)} \varphi^{(0)'} + \left\{ L'(\varphi^{(0)}) \varphi^{(0)'} \frac{\partial}{\partial z} + L\Delta \right\} \mu^{(1)}. \quad (\text{A4})$$

Taking the limit of $L \rightarrow 0+$ naively in Eq. (A4) yields $i\omega \tilde{\varphi}^{(1)} = \tilde{V}_z^{(1)} \varphi^{(0)'}$. This is differentiated with respect to z to give $\partial\tilde{V}_z^{(1)}/(\partial z) \rightarrow 0$ as $z \rightarrow 0+$ unless h vanishes because of Eqs. (17) and (18). It is impossible, however, to impose this boundary condition for any nonzero h because Eq. (A3) has two other boundary conditions. For $h \neq 0$, the second term on the rhs of Eq. (A4) cannot be neglected, even when L is sufficiently small, because of a steep change of $\mu^{(1)}$ inside the boundary layer. Thus, $i\omega \tilde{\varphi}^{(1)} = \tilde{V}_z^{(1)} \varphi^{(0)'}$ holds only outside the boundary layer.

Suppose $h \neq 0$. As L becomes smaller, to satisfy both Eqs. (19) and (A4), the magnitude of $\mu^{(1)}$ becomes larger near $z = 0$. In the limit of $L \rightarrow 0+$, considering the Fourier transform of Eq. (16), $\mu^{(1)}$ and $\partial^2 \tilde{\varphi}^{(1)}/(\partial z^2)$ are

likewise singular at the interface, while $\partial\tilde{\varphi}^{(1)}/(\partial z)$ is finite there, considering that of Eq. (17). For simplicity, we use the thickness of the boundary layer, Δ . It decreases to zero as L becomes smaller, which we can check simply by deriving a differential equation with respect to the real part of Q from Eq. (59) of Ref. 28 and neglecting the small inhomogeneous term to consider the equation within the boundary layer. Integrating the Fourier transform of Eq. (16) from $z = 0$ to Δ , we find

$$\left[M_0 \lim_{z \rightarrow \Delta+} \frac{\partial}{\partial z} \tilde{\varphi}^{(1)} \right]_0^\Delta = - \int_0^\Delta dz \tilde{\mu}^{(1)} \quad (\text{A5})$$

in the limit of $L \rightarrow 0+$, *i.e.*, $\Delta \rightarrow 0+$. Unless h vanishes, the rhs of Eq. (A3) is affected by the singular behavior of $\tilde{\mu}^{(1)}$ in the limit of $L \rightarrow 0+$, but $\partial\tilde{V}_z^{(1)}/(\partial z)$ remains finite at the interface. Thus, we find

$$\lim_{z \rightarrow 0+} \tilde{V}_z^{(1)} = \lim_{\Delta \rightarrow 0+} \lim_{z \rightarrow \Delta+} \tilde{V}_{z \text{ out}}^{(1)}, \quad (\text{A6})$$

which can be also derived from Eq. (29). As stated above, $\partial\tilde{\varphi}^{(1)}/(\partial z)$ remains finite in the boundary layer when L decreases to approach zero. Integrating the derivative from $z = 0$ to Δ and taking the limit of $L \rightarrow 0+$ give the first equality of

$$\lim_{z \rightarrow 0+} \tilde{\varphi}^{(1)} = \lim_{\Delta \rightarrow 0+} \lim_{z \rightarrow \Delta+} \tilde{\varphi}_{\text{out}}^{(1)} = \frac{h}{M_{00}} \tilde{\zeta}^{(1)}, \quad (\text{A7})$$

the second equality of which comes from Eqs. (3), (18), (32) and (A6). Similarly, $\tilde{\varphi}^{(1)}$ equals $-h\tilde{\zeta}^{(1)}/M_{00}$ in the limit of $z \rightarrow 0-$.

Appendix B: Solution of Eq. (60).

In the complex plane of θ , Eq. (60) has regular singular points at $\theta = 0$, 1, and ∞ . Around $\theta = 0$, the linearly independent solutions are given by

$$\begin{aligned} f_{01}(\theta) &\equiv \mathcal{F}(a, b, a+b, \theta) \quad \text{and} \\ f_{02}(\theta) &\equiv \theta^{1-a-b} \mathcal{F}(1-a, 1-b, 2-a-b, \theta). \end{aligned} \quad (\text{B1})$$

Each can be analytically continued to the solution around $\theta = 1$, and to the solution around $\theta = \infty$. Two linearly independent solutions in the latter region can be taken so that one has a factor θ^{-a} and the other has θ^{-b} , as shown by Eq. (15.3.7) of Ref. 56. Because of the boundary condition at $\theta \rightarrow \infty$ and $a < 0 < b$, we arrive at the first line of Eq. (61). For this first line, we write $f_\infty(\theta)$, which diverges logarithmically as $\theta \rightarrow 1$ as shown by Eqs. (B7) and (B8) below. We have only to look at the real axis of θ on the positive side, which is covered by the circles of the convergence with partial overlapping.

If we have $\Lambda^2 \leq 1$, θ cannot be smaller than the unity, the logarithmic singularity does not matter and $g(\theta)$ need

not be defined for $0 < \theta < 1$. Let us consider the case of $\Lambda^2 > 1$. The path of the analytical continuation runs through the upper half (with the positive imaginary part) of the complex θ -plane or through the lower half (with the negative imaginary part). For the results obtained by way of these paths, we respectively write

$$\begin{aligned} f_0^+(\theta) &= B_1^+ f_{01}(\theta) + B_2^+ f_{02}(\theta) \text{ and} \\ f_0^-(\theta) &= B_1^- f_{01}(\theta) + B_2^- f_{02}(\theta) \end{aligned} \quad (\text{B2})$$

for $|\theta| < 1$. Using Eq. (15.3.7) of Ref. 56, we have

$$\begin{aligned} B_1^\pm &\equiv \frac{\Gamma(2-a-b)\Gamma(b-a)}{J\Gamma(1-a)^2} e^{\mp i\pi b} \text{ and} \\ B_2^\pm &\equiv \frac{\Gamma(a+b)\Gamma(b-a)}{J\Gamma(b)^2} e^{\pm i\pi a}, \end{aligned} \quad (\text{B3})$$

where Γ denotes the gamma function and we use

$$\begin{aligned} J &\equiv \Gamma(2-a-b)\Gamma(b-a)\Gamma(a+b)\Gamma(a-b) \\ &\times \{\sin^2(\pi a) - \sin^2(\pi b)\} \pi^{-2}. \end{aligned} \quad (\text{B4})$$

Because of the logarithmic divergence at $\theta = 1$, $f_0^+(\theta)$ and $f_0^-(\theta)$ for $0 < \theta < 1$ are not real and are complex conjugates of each other. The second line of Eq. (61) is thus real, as is required.

When Λ^2 is smaller than the unity, we can replace g by f_∞ in Eq. (62). Then, the product of the rhs of Eq. (62) and $(1+K)/(K\Lambda^2)$ turns out to be

$$-\frac{\mathcal{F}(1+b, 2-a, 2+b-a, \Lambda^2)}{\mathcal{F}(1-a, b, 1+b-a, \Lambda^2)} \quad (\text{B5})$$

with the aid of Eq. (15.2.1) of Ref. 56. The above tends to $1/(\Lambda^2 - 1)$ as K is smaller, considering Eq. (15.1.8) of Ref. 56 and Eq. (59). We use this approximate expression for small K in Eqs. (40) and (54) to find d_1 to vanish. It is thus reasonable that d_1 almost vanishes for $\Omega^2 > 1$ in Fig. 3, where K is much smaller than the unity. It is to be noted that we cannot fulfill the boundary conditions stated below Eq. (57) by putting K equal to zero naively in Eq. (57).

Using the digamma function Ψ , we define $\mathcal{G}_{ab}(\theta)$ as

$$\begin{aligned} \sum_{k=0}^{\infty} \frac{\Gamma(a+k)\Gamma(b+k)}{(k!)^2\Gamma(a)\Gamma(b)} (1-\theta)^k \{ \Psi(a+k) - \Psi(a) \\ + \Psi(b+k) - \Psi(b) - 2\Psi(1+k) + 2\Psi(1) \}. \end{aligned} \quad (\text{B6})$$

Let us write \mathcal{F}_c for $\mathcal{F}(a, b, c, 1-\theta)$. For $0 < \theta < 1$, $f_{01}(\theta)$ equals

$$\begin{aligned} &\frac{-\Gamma(a+b)}{\Gamma(a)\Gamma(b)} [\mathcal{G}_{ab}(\theta) + \mathcal{F}_1 \ln(1-\theta) \\ &+ \{ \Psi(a) + \Psi(b) - 2\Psi(1) \} \mathcal{F}_1] , \end{aligned} \quad (\text{B7})$$

while $f_{02}(\theta)$ equals

$$\begin{aligned} &\frac{-\Gamma(2-a-b)}{\Gamma(1-a)\Gamma(1-b)} [\mathcal{G}_{ab}(\theta) + \mathcal{F}_1 \ln(1-\theta) \\ &+ \{ \Psi(1-a) + \Psi(1-b) - 2\Psi(1) \} \mathcal{F}_1] . \end{aligned} \quad (\text{B8})$$

We perform two separate operations of $(\partial/\partial a) + (\partial/\partial b)$ and $\partial/\partial c$ on Kummer's formula, $\mathcal{F}_c = \theta^{(c-a-b)} \mathcal{F}(c-a, c-b, c, 1-\theta)$, which is given by Eq. (15.3.3) of Ref. 56. We combine the two results of the operations in the limit of $c \rightarrow 1$ to find $\mathcal{G}_{ab}(\theta) = \mathcal{G}_{1-a, 1-b}(\theta) \theta^{1-a-b}$, which we use to relate Eqs. (B7) and (B8) with Eq. (15.3.10) of Ref. 56. Because they are valid when the absolute value of the argument of $1-\theta$ is smaller than π , we find how to interpret Eqs. (B7) and (B8) for $1 < \theta < 2$. When $f_{01}(\theta)$ and $f_{02}(\theta)$ are analytically continued to the region $|1-\theta| < 1$ by way of the upper half plane of θ , *i.e.*, the lower half plane of $1-\theta$, they respectively becomes Eqs. (B7) and (B8) with $\ln(1-\theta)$ being replaced by $\ln(\theta-1) - i\pi$. It should be replaced by $\ln(\theta-1) + i\pi$ when the path runs through the lower half plane of θ . By these respective ways, we can continue f_0^+ and f_0^- analytically to the region of $|1-\theta| < 1$. Both the results agree with $f_\infty(\theta)$ if $|\theta| > 1$ is also satisfied.

Appendix C: Some details in Sec. V C.

When τ is sufficiently small, we substitute Eq. (80) with $s \gg 1$ into the integral of Eq. (101) to obtain

$$D(k) \approx \frac{k_B T_c k^2}{9u^* \xi_0^3} \int_0^\infty dz e^{-2kz} (s\tau)^{\nu d} \quad (\text{C1})$$

with the aid of the hyperscaling law $2\beta + \gamma = \nu d$. Because of Eqs. (89) and (96), we have

$$(s\tau)^\beta \approx \left(\frac{\sqrt{6}\beta\xi_0}{\nu(z+l)} \right)^{\beta/\nu}, \quad (\text{C2})$$

which is substituted into Eq. (C1) to give

$$D(k) \approx \frac{\sqrt{6}\beta k_B T_c k^2}{2\nu\pi^2 \xi(0+)^2} e^{2kl} \int_1^\infty dz_1 e^{-2klz_1} z_1^{-3} \quad (\text{C3})$$

with the aid of Eq. (93). The exponential integral above tends to $1/2$ as kl becomes small, which leads to Eq. (104).

In Sec. V C, we use d_0 defined by Eq. (49) in the Gaussian model. However, by regarding ξ_c as $\xi(0+)$, we can redefine d_0 from D in Eq. (99) so that the definition remains unchanged in the regime of the Gaussian model and is valid beyond its regime. Using Eq. (27) and comparing Eq. (48) with Eq. (99), the redefinition is given so that we have

$$D(k) = \frac{c_b}{\xi(0+)^4} \lambda^2 d_0 (k\xi(0+)) , \quad (\text{C4})$$

which is reduced to the lhs of Eq. (103) in the regime of the Gaussian model. When $s(0+)$ is much larger than the unity, we can write $\psi''(0+)$ in terms of $\psi'(0+)$ by using Eq. (96). Using this result in Eq. (22), we then find

$$\lambda^2 \approx \frac{h^2 \xi(0+)^3}{6c_b M_{00}} \left(1 + \frac{\nu}{\beta}\right)^2 \quad (C5)$$

with the aid of Eqs. (76) and (93). Noting the definition of Θ given below Eq. (82) and $2\beta = \nu\eta + \nu$ stated below Eq. (105), we use Eqs. (70), (86), and (88) to rewrite the factor before the parentheses above and find

$$\lambda^2 \approx \frac{k_B T_c}{24\pi^2 c_b} \left(1 + \frac{\nu}{\beta}\right)^2 \quad (C6)$$

for sufficiently small τ . Equation (C6) is independent of h , but does not contradict with $\lambda = 0$ for $h = 0$ because, as mentioned below Eq. (104), $s(0+) \gg 1$ cannot occur when h vanishes. When τ is sufficiently small, we substitute Eqs. (104) and (C6) into Eq. (C4) to obtain

$$d_0(k\xi(0+)) \approx \frac{6\sqrt{6}\beta}{\nu} \left(1 + \frac{\nu}{\beta}\right)^{-2} \{k\xi(0+)\}^2 \quad (C7)$$

for small $k\xi(0+)$. The factor before the brackets above is about 0.9. Thus, we find Eq. (49) roughly valid for small K and small τ . It is to be noted that, in contrast with λ , Λ is approximately proportional to h for sufficiently small τ because of Eqs. (27), (105), and (C6). For sufficiently small τ , we find that $D(k)$ for small k is approximately proportional to $h^{4/3}$ from Eqs. (104) and (105). This is consistent with the fact that Eq. (99) is valid up to the order of Λ^3 .

In the Gaussian model, as shown in Fig. 3, the curve of d_1 has a peak located at $\Omega^2 = 1$. As discussed below Eq. (98), the peak of d_1 would be at $\Omega^2 = \Xi(0+)^2$ in general. We use Eqs. (26), (93) and (96) to find

$$\Xi(0+)^2 \approx \frac{6\beta^2}{(\beta + \nu)^2} \approx 0.7 \quad (C8)$$

when τ is small enough to give $s(0+) \gg 1$. Thus, the peak is not so much shifted as τ becomes sufficiently small. Still then, d_1 vanishes in the limit of $\Omega^2 \rightarrow 0$ because of Eqs. (55), (102), and (C4); it tends to about $-1/2$ as Ω^2 approaches zero, as shown in Appendix D. Thus, if K is interpreted as $k\xi(0+)$ and d_0 is redefined as above, for sufficiently small τ we can expect Eq. (64) and the discussion on the intersection at the outset of the sixth paragraph in Sec. IV B to hold. Thus, Eq. (107) would be valid when $4\lambda^2 \ll \{k\xi(0+)\}^3$ holds together with $k\xi(0+) \ll 1$.

Appendix D: The value of $d_1(K, 0+)$ for small K .

In the fourth paragraph of Sec. IV B, we show $d_1(K, 0+) \rightarrow -1/2$ in the limit of $K \rightarrow 0+$ by using

the solution of Eq. (57). A simpler, but approximate, discussion to this result is as follows. Suppose that Ω^2 is sufficiently small; Eq. (57) is approximated to be

$$(\partial_Z^2 - K^2)U_{\text{out}} = 2\partial_Z U_{\text{out}} \quad (D1)$$

up to a sufficiently large value of Z . At this value, we regard U_{out} as zero instead of imposing the boundary condition of $U_{\text{out}} \rightarrow 0$ as $Z \rightarrow \infty$. We thus use Eq. (37) to obtain $U_{\text{out}}(Z) = e^{(1-K_1)Z}$, where K_1 is defined below Eq. (58). Substituting this into Eq. (54) with the aid of Eq. (40), we obtain $d_1(K, 0+) \approx -1/2$ for small K .

Let us consider similarly Eq. (98) for sufficiently large Λ^2 . We assume τ to be sufficiently small and neglect the weak dependence of C on ψ . Because of Eqs. (26) and (96), we use $\xi_a = \xi(0+)$ to find

$$\frac{\Xi'}{\Xi} \approx - \left(1 + \frac{\beta}{\nu}\right) \frac{\xi(0+)}{z+l} \quad (D2)$$

for $s \gg 1$. We introduce $Z_0 \equiv l/\xi(0+)$, which approximately equals $\sqrt{6}\beta/\nu$ for small τ because of Eq. (93). We have $2\beta/\nu = 1 + \eta$ as mentioned below Eq. (105). Equation (98) is thus approximated to be

$$(\partial_Z^2 - K^2)U_{\text{out}} = \frac{3+\eta}{Z+Z_0} \partial_Z U_{\text{out}} \quad (D3)$$

up to a sufficiently large value of Z . At this value of Z , we regard U_{out} as zero instead of imposing the boundary condition of $U_{\text{out}} \rightarrow 0$ as $Z \rightarrow \infty$. We thus obtain

$$U_{\text{out}}(Z) \propto (Z + Z_0)^{2+(\eta/2)} \mathcal{K}_{2+(\eta/2)}(K(Z + Z_0)), \quad (D4)$$

where \mathcal{K}_q represents the modified Bessel function. Determining the constant of proportionality by using Eq. (37), we find

$$\lim_{Z \rightarrow 0+} \partial_Z U_{\text{out}} = -K \frac{\mathcal{K}_{1+(\eta/2)}(KZ_0)}{\mathcal{K}_{2+(\eta/2)}(KZ_0)}, \quad (D5)$$

which tends to $-K^2 Z_0 / (2 + \eta)$ as KZ_0 approaches zero. Substituting the above into Eq. (54) with the aid of Eq. (40), we obtain $d_1(K, 0+) \approx (-\eta - 1)/(\eta + 2) \approx -1/2$ for small $KZ_0 = kl$.

Appendix E: Naive average based on Eq. (71).

We here consider the mean square amplitude for modes of small wavenumber by regarding the ambient mixture as a heat and particle bath in the renormalized local functional theory. We define $\tilde{\Omega}$ as Eq. (1) in which M is given by Eq. (70) and f is given by Eq. (71). Suppose that ψ and ζ deviates from Eq. (74) and zero, respectively. We write ψ_1 for the deviation of ψ and below use ψ in the sense of Eq. (74). The resultant deviation of $\tilde{\Omega}$, denoted by $\delta\tilde{\Omega}$, is calculated below up to the second order with

respect to ψ_1 and ζ by means of the same procedure as used in Appendix of Ref. 28. With the aid of Eqs. (14) and (76), we find $\delta\tilde{\Omega}[\psi_1, \zeta]$ to be given by

$$\begin{aligned} & \int_{C^e} d\mathbf{r} \left\{ \left(\frac{f_R''}{2} + \frac{M_0''\psi'^2}{4} \right) \psi_1^2 + M_0'\psi'\psi_1 \frac{\partial\psi_1}{\partial z} \right. \\ & \quad \left. + \frac{M_0|\nabla\psi_1|^2}{2} \right\} + \int d\mathbf{x} \left[|\nabla\zeta|^2 f_s(\varphi^{(0)}(0+)) \right. \\ & \quad \left. + \mathcal{M}_{00}\zeta \left\{ \frac{h\zeta}{M_0} - \psi_1(\mathbf{x}, \zeta+) + \psi_1(\mathbf{x}, \zeta-) \right\} \right], \quad (\text{E1}) \end{aligned}$$

where \mathbf{x} denotes (x, y) , $|\nabla\zeta|^2$ denotes $(\partial\zeta/\partial x)^2 + (\partial\zeta/\partial y)^2$, and \mathcal{M}_{00} is defined as $M_0'(h/M_0)^2 + M_0\psi''$ evaluated at $z = 0$. Equation (E1) becomes Eq. (A9) of Ref. 28 when we use the Gaussian model.

We write $\delta\tilde{\Omega}^+$ for the sum of the $\delta\tilde{\Omega}$ and the contribution from the membrane energy independent of ψ_1 . The membrane energy consists of the bending energy and the energy involving the equilibrium in-plane pressure, $p_m^{(0)}$. In this static theory, the probability density of ψ_1 and ζ is proportional to the Boltzmann weight, $\exp(-\delta\tilde{\Omega}^+/k_B T)$. Integrating this density with respect to ψ_1 yields the probability density of ζ , from which we can find its variance, *i.e.*, the mean square amplitude. Apart from a multiplication constant, we can obtain the result of this integration by replacing $\delta\tilde{\Omega}^+$ by the minimum of $\delta\tilde{\Omega}^+$ for a given ζ in the Boltzmann factor because the probability density considered here is a Gaussian distribution. We write ψ_1^* for ψ_1 minimizing $\delta\tilde{\Omega}^+$, and thus $\delta\tilde{\Omega}$, for a given ζ . The stationary condition of Eq. (E1) with respect to ψ_1 is given by Eq. (16) with its rhs being put equal zero and Eq. (17) if $\varphi^{(1)}$ and $\zeta^{(1)}$ are respectively replaced by ψ_1^* and ζ . Taking the Fourier transforms of the resultant equations with respect to x and y , we consider their components for the wavenumber vector \mathbf{k} . The time variable t need not be specified here. Replacing ψ_1 with ψ_1^* in Eq. (E1), we find the minimum of $\delta\tilde{\Omega}$ to be given by

$$\begin{aligned} & l_p^2 \sum_{\mathbf{k}} \left[k^2 f_s(\varphi^{(0)}(0+)) \hat{\zeta}(-\mathbf{k}) \hat{\zeta}(\mathbf{k}) \right. \\ & \quad \left. + \mathcal{M}_{00} \hat{\zeta}(-\mathbf{k}) \left\{ \frac{h\hat{\zeta}(\mathbf{k})}{M_{00}} - \hat{\psi}_1^*(\mathbf{k}, 0+) \right\} \right]. \quad (\text{E2}) \end{aligned}$$

Introducing $\hat{\psi}_0(\mathbf{k}, z) \equiv -\hat{\zeta}(\mathbf{k})\psi'(z)$, we define $\chi(\mathbf{k}, z)$ as $\hat{\psi}_1^*(\mathbf{k}, z)/\hat{\psi}_0(\mathbf{k}, z)$. Considering the statement below Eq. (33), we use the stationary condition to find $\chi(\mathbf{k}, z) \rightarrow 1$ as k approaches zero,

$$\chi'' + \left(\frac{d}{dz} \ln M_0 \hat{\psi}_0^2 \right) \chi' = k^2 \chi \quad \text{for } z \neq 0, \quad (\text{E3})$$

where the prime indicates the differentiation with respect

to z , and

$$\mathcal{M}_{00}(\chi - 1) = h\chi' \quad \text{at } z \rightarrow 0 \pm. \quad (\text{E4})$$

We below consider $\chi(\mathbf{k}, z)$ for $z > 0$, noting that $\hat{\psi}_1^*(\mathbf{k}, z)$ is odd with respect to z . Up to a given value of $z(> 0)$, we can approximate the rhs of Eq. (E3) to be k^2 for a sufficiently small k . Noting that M_0 equals $C(\psi)$, within this approximation we find

$$\chi'(\mathbf{k}, z) = \frac{\chi_0 - k^2 \int_z^\infty dz' C(\psi(z')) \hat{\psi}_0(\mathbf{k}, z')^2}{C(\psi(z)) \hat{\psi}_0(\mathbf{k}, z)^2}, \quad (\text{E5})$$

where χ_0 is a constant. Because $\hat{\psi}_1(\mathbf{k}, z)$ would decrease monotonically in the region of z considered here, χ_0 should vanish. This leads to χ with a constant of the integration. This constant is determined by Eq. (E4). Hence, we arrive at

$$\begin{aligned} & \hat{\psi}_1^*(\mathbf{k}, 0+) - \frac{h\hat{\zeta}(\mathbf{k})}{M_{00}} \\ & = -\frac{k^2 \hat{\zeta}(\mathbf{k})}{\mathcal{M}_{00}} \int_0^\infty dz' C(\psi(z')) \psi'(z')^2, \quad (\text{E6}) \end{aligned}$$

where we use $\hat{\psi}_0(\mathbf{k}, 0+) = h\hat{\zeta}(\mathbf{k})/M_{00}$. We can substitute Eq. (E6) into Eq. (E2) for sufficiently small k . Adding the terms of the membrane energy, we find the probability density of $\hat{\zeta}(\mathbf{k})$. For a tensionless membrane, the term involving f_s in Eq. (E2) cancels with the term involving $p_m^{(0)}$ because of Eq. (43), and the mean square amplitude for sufficiently small k turns out to be Eq. (53) with the second term in the brackets being replaced by

$$2k^2 \int_0^\infty dz C(\psi(z)) \psi'(z)^2. \quad (\text{E7})$$

The corresponding term in Eq. (107) is $2D$, and is asymptotic to the double of Eq. (E7) as k is smaller, judging from Eq. (100).

Differentiating Eq. (14) with respect to $\mu(\mathbf{r})$, we obtain the two-point susceptibility and find M_0/N to be comparable with the square of the local correlation length. As mentioned above, Eq. (16) and the differential equation of the stationary condition share the same operator. It is thus appropriate that the Fourier transform of the latter is nondimensionalized in terms of the local correlation length. Considering that χ is determined by the boundary condition at $z = 0+$, Eq. (E4), the approximation introduced above Eq. (E5), and thus Eq. (E7), should be valid when $k\xi(0+) \ll 1$ holds. In the Gaussian model, Eqs. (E3) and (E4) are solved exactly to yield $\chi(\mathbf{k}, z) = e^{(1-K_1)z}/K_1$, which leads to Eq. (A11) of Ref. 28.

-
- [1] P. B. Canham, *J. Theoret. Biol.* **26**, 61 (1970).
- [2] W. Helfrich, *Z. Naturforsch., Teil C* **28**, 693 (1973).
- [3] S. J. Singer and G. L. Nicolson, *Science* **175**, 720 (1972).
- [4] F. Brochard and J. F. Lennon, *J. Phys. (Paris)* **11**, 1035 (1975).
- [5] F. Brochard, P. G. de Gennes, and P. Pfeuty, *J. Phys. (Paris)* **37**, 1099 (1976).
- [6] C. Tanford, *Proc. Natl. Acad. Sci. USA* **76**, 3318 (1979).
- [7] F. Jähnig, *Biophys. J* **71**, 1348 (1996).
- [8] W. Helfrich, in *Les Houches 1988, Session XLVIII, Liquids at Interfaces*, edited by J. Charvolin, J. F. Joanny, and J. Zinn-Justin (North-Holland, Amsterdam, 1990).
- [9] D. Sornette and N. Ostrowsky, in *Micelles, Membranes, Microemulsions, and Monolayers*, edited by W. M. Gilbert, A. Ben-Shaul, and D. Roux (Springer, New York, 1994).
- [10] W. Helfrich, *Z. Naturforsch., Teil C* **30**, 841 (1975).
- [11] P. G. de Gennes and C. Taupin, *J. Phys. Chem.* **86**, 2294 (1982).
- [12] P. G. de Gennes, F. Brochard-Wyart, and D. Quéré, *Capillarity and Wetting Phenomena* (Springer, New York, 2004), Chap. 8.2.
- [13] D. Roux and A. M. Bellocq, in *Physics of Amphiphiles*, edited by V. Degiorgio and M. Corti (North Holland, Amsterdam, 1985), p. 842.
- [14] O. Diat, D. Roux, and F. Nallet, *J. Phys. II (France)* **3**, 1427 (1993).
- [15] J. Yamamoto and H. Tanaka, *Nat. Mater.* **4**, 75 (2004).
- [16] W. Helfrich, *Z. Naturforsch., Teil A* **33**, 305 (1978).
- [17] J. O. Indekeu, P. J. Upton, and J. M. Yeomans, *Phys. Rev. Lett.* **61**, 2221 (1988).
- [18] P. J. Upton, J. O. Indekeu, and J. M. Yeomans, *Phys. Rev. B* **40**, 666 (1989).
- [19] A. J. Liu and M. E. Fisher, *Phys. Rev. A* **40**, 7202 (1989).
- [20] A. Hanke and S. Dietrich, *Phys. Rev. E* **59**, 5081 (1999).
- [21] R. Okamoto and A. Onuki, *J. Chem. Phys.* **136**, 114704 (2012).
- [22] This correlation length should be estimated near the impurity, judging from the discussion in the fifth paragraph of Sec. V C.
- [23] A. Furukawa, A. Gambassi, S. Dietrich, and H. Tanaka, *Phys. Rev. Lett.* **111**, 055701 (2013).
- [24] Y. Fujitani, *J. Phys. Soc. Jpn.* **83**, 024401 (2014); **83**, 108001 (2014) [erratum].
- [25] Y. Fujitani, *J. Phys. Soc. Jpn.* **83**, 084401 (2014).
- [26] Y. Fujitani, *J. Phys. Soc. Jpn.* **82**, 124601 (2013); **83**, 088001 (2014) [erratum].
- [27] R. Okamoto, Y. Fujitani, and S. Komura, *J. Phys. Soc. Jpn.* **82**, 084003 (2013).
- [28] Y. Fujitani, *Phys. Rev. E* **91**, 042402 (2015).
- [29] A. J. Bray and M. A. Moore, *J. Phys. A: Math. Gen.* **10**, 1927 (1977).
- [30] M. N. Binder, in *Phase Transition and Critical Phenomena VIII*, edited by C. Domb and J. L. Lebowitz, (Academic, London 1983).
- [31] W. H. Diehl, in *Phase Transition and Critical Phenomena X*, edited by C. Domb and J. L. Lebowitz, (Academic, London 1986).
- [32] T. W. Burkhardt and H. W. Diehl, *Phys. Rev. B* **50**, 3894 (1994).
- [33] W. H. Diehl, *Int. J. Mod. Phys. B* **11**, 3503 (1997).
- [34] W. H. Diehl, *Ber. Bunsenges, Phys. Chem.* **98**, 466 (1994).
- [35] M. E. Fisher and P. G. de Gennes, *C. R. Acad. Sci. B* **287**, 207 (1978).
- [36] J. Rudnick and D. Jasnow, *Phys. Rev. Lett* **48**, 1059 (1983).
- [37] M. Smock, H. W. Diehl, and D. P. Landau, *Ber. Bunsenges, Phys. Chem.* **98**, 486 (1994).
- [38] H. Nakanishi and M. E. Fisher, *Phys. Rev. Lett* **49**, 1565 (1982).
- [39] J. W. Cahn, *J. Chem. Phys.* **66**, 3667 (1977).
- [40] H. W. Diehl and M. Smock, *Phys. Rev. B* **47**, 5841 (1993).
- [41] R. Okamoto and A. Onuki, *Phys. Rev. E* **88**, 022309 (2013).
- [42] A. Onuki, *Phase Transition Dynamics*, (Cambridge University Press, Cambridge, England, 2002), Chaps. 4 and 6.
- [43] P. C. Hohenberg and B. I. Halperin, *Rev. Mod. Phys.* **49**, 435 (1977).
- [44] The singularity in the limit of zero viscosity does not influence Eq. (A4).
- [45] Equation (7) is the same as Eq. (10) of Ref. 28, Eq. (12) of which remains valid here.
- [46] Ou-Yang Zhong-can and W. Helfrich, *Phys. Rev. Lett.* **59**, 2486 (1987).
- [47] Ou-Yang Zhong-can and W. Helfrich, *Phys. Rev. A* **39**, 5280 (1989).
- [48] U. Seifert and S. A. Langer, *Europhys. Lett.* **23**, 71 (1993).
- [49] Y. Fujitani, *Physica A* **203**, 214 (1994); **237**, 346(E) (1997).
- [50] Y. Fujitani, *J. Chem. Phys.* **116**, 7787 (2002).
- [51] T. R. Powers, *Rev. Mod. Phys.* **82**, 1607 (2010).
- [52] C. M. Bender and S. A. Orszag, *Advanced Mathematical Methods for Scientists and Engineers*, (Springer, New York, 1999), Chaps. 1.5 and 9.2.
- [53] In Ref. 28, the last term in the braces on the rhs of Eq. (33) cancels with the second term, while the Fourier transform of the sum of the first two terms in the braces equals the first term on the lhs of Eq. (67).
- [54] B. Alberts, A. Johnson, J. Lewis, M. Raff, K. Roberts, and P. Walter, *Molecular Biology of the Cell*, (Garland, New York, 2008), Chap. 10.
- [55] A. Erdélyi (ed.), *Higher Transcendental Functions, vol. I*, (McGraw-Hill, New York, 1953), Chap. 2.
- [56] M. Abramowitz and I. A. Stegun, *Handbook of Mathematical Functions*, (Dover, New York, 1964), Chap. 15.
- [57] J. S. Rowlinson and B. Widom, *Molecular Theory of Capillarity*, (Clarendon Press, UK, 1982), Chapters 3, 4.6, and 9.1-2.
- [58] C. I. Poser and I. C. Sanchez, *Macromolecules* **14**, 361 (1981).
- [59] B. S. Carley, L. E. Scriven, and H. T. Davis, *AIChE J.* **26**, 705 (1980).
- [60] H. Kahl and S. Enders, *Phys. Chem. Chem. Phys.* **4**, 931 (2002).
- [61] P. M. W. Cornelisse, C. J. Peters and J. de Swaan Arons, *Fluid Phase Equilib.* **117**, 312 (1996).
- [62] I. Iwanowski, K. Leluk, M. Rudowski, and U. Kaatz, *J. Phys. Chem. A* **110**, 4313 (2006).

- [63] The term " $f(\varphi) - \mu^{(0)}\varphi + \text{constant}$ " corresponds with Eq. (71) and $\mu^{(0)}$ does not vanish. The chemical potential in the ψ^4 theory, denoted by μ_∞ in Ref. 21, vanishes in the critical fraction.
- [64] Assuming f_s to be a linear function here should amount to assuming the bare value of the surface enhancement to be positive in the previous renormalization group theory, judging from Ref. 33 and Eq. (3.95) of Ref. 31.
- [65] N. Lei and X. Lei, *Langmuir* **14**, 2155 (1998).